이학석사 학위논문

Guanidine Cyclic Diimides: Structure and Reactivity

구아니딘 고리형 다이이미드: 구조 및 반응성

2018년 8월

서울대학교 대학원

화학부 생화학 전공

안 태 양

Guanidine Cyclic Diimides: Structure and Reactivity

지도교수 이 연

이 논문을 이학석사 학위논문으로 제출함

2018년 8월

서울대학교 대학원
화학부 생화학 전공
안 태 양

안태양의 석사학위논문을 인준함
2018년 8월

위 원 장 이 홍 근 (인)
부 위 원 장 이 연 (인)
위 원 홍 종 인 (인)

Abstract

Guanidine Cyclic Diimides: Structure and Reactivity

Taeyang An
Department of Chemistry
College of Natural Science
Seoul National University

Among various chemical structures that can be obtained with the nucleophilic reaction of guanidines, imide-like structures have been rarely reported until now. The reason is probably because many researchers believe that guanidine is a stronger base but a weaker nucleophile than amines and that imide formation often requires harsh anhydrous conditions at elevated temperatures to facilitate the dehydration.

In this paper, I report that unique structures of guanidine cyclic diimides (GCDIs) can be readily formed under mild reaction conditions at ambient temperatures for the first time. Unexpectedly, GCDI structures were obtained as major products in the reaction between guanidine and cyclic anhydride in high yields. Along with NMR data, the single crystal X-ray diffraction data clearly represented the GCDI structure with two succinimide rings formed on different nitrogen atoms of guanidine. Two succinimide rings were shown to be almost perpendicular to each other, suggesting disruption of the delocalized π-orbitals. The C-N bond lengths of the central guanidine in the

GCDI structure were significantly changed. The two succinimide rings seemed to rotate freely at room temperature.

The degradation property of the GCDI structure was also very different from that of amine-based imides. The GCDI structure was stable in aprotic solvents for several weeks at least, however, it rapidly degraded into corresponding amides and finally, into original guanidine in protic solvents, e.g. water and methanol. The degradation was accelerated in both acidic and basic conditions. The guanidine-based imides form as well as degrade in much milder conditions than typical amine-based imides do, probably owing to charge-delocalization ability of guanidine structure.

Keywords: Guanidine cyclic diimide (GCDI), *gauche* conformation, solvolysis, charge-delocalized intermediates
Student Number: 2016-29102

Contents

1. Introduction

Guanidine is frequently employed as a nucleophilic reagent and catalyst in various reactions. Many biologically important compounds such as creatine phosphate, tetrodotoxin, amiloride, and rosuvastatin have been synthesized by nucleophilic reactions of guanidine under natural or artificial conditions (1-4). Arginine, one of the most abundant guanidine-based molecules available in nature, can be phosphorylated in the body or acylated for the synthesis of artificial peptides through reactions with corresponding electrophiles (5-8). However, imide-like guanidine-based structures have been rarely reported, (9) probably because many researchers believe that guanidine is a stronger base but a weaker nucleophile than most amines due to its delocalized π-orbitals (10) and that imide formation often requires harsh anhydrous conditions at elevated temperatures to facilitate the dehydration of amic acid intermediates (11, 12). I had also originally envisioned that the formation of imide-like structures from guanidine moieties by reaction with cyclic anhydrides is difficult. Unexpectedly, I found that unique guanidine cyclic diimide (GCDI) structures can be readily formed by reactions at ambient temperatures. Herein, I report the structural and reactive properties of the GCDI structure for the first time.

2. Materials and Methods

2.1. Synthetic Procedures

2.1.1. Reagents and Materials

N,*N*-dimethylformamide (DMF), acetonitrile (ACN), dichloromethane (DCM), succinic anhydride, phthalic anhydride, glutaric anhydride, 1-hydroxybenzotriazole hydrate (HOBt), *N*-(3-dimethylaminopropyl)-*N'*-ethylcarbodiimide hydrochloride (EDC·HCl), butylamine, pyridine, trifluoroacetic acid (TFA) and potassium dideuterium phosphate were purchased from Sigma-Aldrich (USA). Piperidine and 1*H*-pyrazole-1-carboxamidine hydrochloride were purchased from Alfa Aesar (USA). *N*,*N*-diisopropylethylamine (DIPEA), *cis*-1,2-cyclohexanedicarboxylic anhydride, allylsuccinic anhydride, 4-bromophthalic anhydride and phenylsuccinic anhydride were purchased from TCI (Japan). Fmoc-Arg(Pbf)-OH was purchased from BeadTech (Korea). Acetic anhydride and triethylamine (TEA) were purchased from Samchun (Korea). Potassium carbonate anhydrous was purchased from Daejung (Korea). $CDCl_3$, D_2O, CD_3OD and d^6-DMSO were purchased from BK Instruments (Korea). All reagents were used without further purification.

Bruker Avance DPX-300 (300 MHz) was used for ^1H-, ^{13}C-NMR analysis, and degradation studies of GCDIs. Varian NMR System 500 MHz (500 MHz) was used for ^1H-, ^{13}C-NMR, gCOSY, HSQC analysis, and degradation studies of GCDIs. Agilent 6100 Series LC/MS, LC (Agilent 1260 infinity), MS (Agilent 6120 Quadrupole LC/MS) was used for LRMS analysis.

2.1.2. Preparation of Butylguanidine Hydrochloride (**1a**)

To a stirred solution of 1*H*-pyrazole-1-carboxamidine hydrochloride

(1.343 g; 9.16 mmol) and DIPEA (1.76 ml; 10.08 mmol) in 10 ml of ACN, butylamine (1.00 ml; 10.08 mmol) was added. The reaction mixture was stirred at an ambient temperature for 21 h and concentrated under reduced pressure. The crude mixture was diluted with deionized water and washed with DCM three times. The aqueous layer was collected and lyophilized. Resulted solid was further washed with diethyl ether and dried *in vacuo* (1.371 g, 99%).

2.1.3. Optimization of GCDI **3aa** Preparation

To a stirred solution of butylguanidine hydrochloride (**1a**) (100 mg; 0.659 mmol) and succinic anhydride in DMF (5 ml), base was added. The reaction mixture was further stirred at various temperatures for 24 h and concentrated under reduced pressure. The crude mixture was diluted with 50 ml of EA and 50 ml of aqueous HCl (0.01 M) and the organic layer was further washed with 50 ml of brine twice. Residual water was removed with anhydrous $MgSO_4$. The product was purified by flash column chromatography (SiO_2, hexane/EA).

2.1.4. General Procedure for GCDI Preparation (**3aa**-**3af**)

To a mixture of butylguanidine hydrochloride (**1a**) (100 mg; 0.659 mmol; 1 equiv.), acid anhydride (3.96 mmol; 6 equiv.) and K_2CO_3 (0.659 mmol; 1 equiv.), DMF (5 ml) was added. The reaction mixture was stirred at 30 °C for 24 h and concentrated under reduced pressure. The crude mixture was diluted with 50 ml of EA and 50 ml of aqueous HCl (0.01 M) and the organic layer was further washed with 50 ml of brine twice. Residual water was removed with anhydrous $MgSO_4$. The product was purified by flash column chromatography (SiO_2, hexane/EA).

2.1.5. Preparation of Ac-Arg-NH-(*n*-Bu)·TFA (**1b**)

2.1.5.1. Synthesis of Fmoc-Arg(Pbf)-NH-(*n*-Bu) (**4**)

To a stirred solution of Fmoc-Arg(Pbf)-OH (2.000 g; 3.08 mmol; 1.2 equiv.), EDC·HCl (709 mg; 3.7 mmol; 1.2 equiv.), and HOBt (500 mg; 3.7 mmol; 1.2 equiv.) in 20 ml of DCM, butylamine (0.36 ml; 3.7 mmol; 1.2 equiv.) was added. The reaction mixture was stirred at an ambient temperature for 3 h and concentrated under reduced pressure. The reaction mixture was diluted with 50 ml of EA and 50 ml of saturated aq. NH_4Cl and the organic layer was further washed with 50 ml of brine twice. Residual water was removed with anhydrous $MgSO_4$. The product was purified by flash column chromatography (SiO_2, hexane/EA) and pale yellow solid was yielded (1.921 g, 89%).

2.1.5.2. Synthesis of H-Arg(Pbf)-NH-(*n*-Bu) (**5**)

To a stirred solution of Fmoc-Arg(Pbf)-NH-(*n*-Bu) (1.500 g; 2.13 mmol; 1.0 equiv.) in DCM (20 ml), piperidine (1.05 ml; 10.5 mmol; 5.0 equiv.) was added. The reaction mixture was stirred at ambient temperature for 24 h and concentrated under reduced pressure. The product was purified by flash column chromatography (SiO_2, EA/MeOH) and pale yellow solid was yielded (906.5 mg, 88%).

2.1.5.3. Synthesis of Ac-Arg(Pbf)-NH-(*n*-Bu) (**6**)

To a stirred solution of H-Arg(Pbf)-NH-(*n*-Bu) (500 mg; 1.04 mmol; 1.0 equiv.) in DCM (10 ml), acetic anhydride (0.12 ml; 1.25 mmol; 1.2 equiv.) and TEA (0.17 ml; 1.25 mmol; 1.2 equiv.) was added. The reaction mixture was stirred at ambient temperature for 24 h and concentrated under reduced pressure. The reaction mixture was diluted with 50 ml of EA and 50 ml of saturated aq. NH_4Cl and the organic layer was further washed with 50 ml of brine twice.

Residual water was removed with anhydrous $MgSO_4$. The product was purified by flash column chromatography (SiO_2, hexane/EA) and white solid was yielded (414.8 mg, 76%).

2.1.5.4. Synthesis of Ac-Arg-NH-(*n*-Bu)·TFA (**1b**)

To a stirred solution of Ac-Arg(Pbf)-NH-(*n*-Bu) (200 mg; 0.382 mmol) in DCM (2.5 ml), TFA (2.5 ml) was added. The reaction mixture was stirred at ambient temperature for overnight and concentrated under reduced pressure. The crude mixture was diluted with deionized water, washed with DCM three times and the aqueous layer was lyophilized. After lyophilizing, the product was further washed with diethyl ether, dried *in vacuo* and orange-colored solid was yielded (141.8 mg, 96%).

2.1.6. Preparation of **3ba**

To a mixture of **1b** (126.3 mg; 0.343 mmol; 1.0 equiv.), succinic anhydride (207.9 mg; 2.057 mmol; 6.0 equiv.), and K_2CO_3 (47.6 mg; 0.343 mmol; 1.0 equiv.), DMF (3 ml) was added. The reaction mixture was stirred at 30 °C for 24 h and concentrated under reduced pressure. The crude mixture was diluted with 30 ml of EA and 30 ml of aqueous HCl (0.01 M) and the organic layer was further washed with 30 ml of brine twice. Residual water was removed with anhydrous $MgSO_4$. The product was purified by flash column chromatography (SiO_2, EA/acetone) and white solid was yielded (33.7 mg, 23%).

2.2. NMR spectroscopy

The ^{1}H- and ^{13}C-NMR spectra were recorded on Bruker Avance DPX-300 or Varian NMR System 500 MHz spectrometers operating

at either 300 or 500 MHz. ^{1}H chemical shifts were referenced from the chemical shifts of tetramethylsilane (for spectra recorded in $CDCl_3$; 0.00 ppm) or residual solvent peaks (for spectra recorded in D_2O; 4.79 ppm). ^{13}C-NMR spectra were recorded with complete proton decoupling. ^{13}C chemical shifts were referenced from the chemical shifts of $CDCl_3$ (77.16 ppm).

Two-dimensional NMR spectra were only recorded for compound **3aa** on Varian NMR System 500 MHz spectrometer. 2D ^{1}H-^{1}H homonuclear and ^{1}H-^{13}C heteronuclear experiments [2D correlated spectroscopy (COSY) and heteronuclear single quantum coherence (HSQC)] were performed.

All spectral data were processed with the MestReNova (Version 6.0.2).

2.3. Degradation Studies of Compounds 3aa, 3ab and 3ac

Degradation of each compound was measured by ^{1}H-NMR spectroscopy. Each compound was dissolved in deuterated solvents ($CDCl_3$, d^6-DMSO, D_2O, CD_3OD, and 250 mM pD 3.1, 5.5, 7.5, and 9.6 deuterated phosphate buffer) at the concentration of about 5 mg/ml. The solution was incubated at 37 °C and at several time points, ^{1}H-NMR spectra were recorded on Bruker Avance DPX-300 (300 MHz) or Varian NMR System 500 MHz (500 MHz) spectrometer.

2.4. Single Crystal X-Ray Diffraction (SC-XRD)

2.4.1. Crystallization of Compound **3aa**

33.3 mg of **3aa** was dissolved in 0.5 ml of DCM. 2 ml of hexane was added and turbidity was observed. The mixture was vortexed and filtered. The resulting filtrate was incubated at ambient

temperature. After 4 h-incubation, crystal formation was observed and the vessel was sealed.

2.4.2. X-Ray Crystallographic Analysis

All data were collected on a Bruker SMART APEX II ULTRA diffractometer equipped with multilayer monochromated Mo Kα radiation (λ = 0.710 73 Å) generated by a rotating anode. The cell parameters for the compounds were obtained from a least-squares refinement of the spot (from 36 collected frames). Data collection, data reduction, and multi-scan absorption correction were carried out using the software package APEX2 (13). All of the calculations for the structure determination were carried out using the SHELXTL package (14).

2.5. DFT Analysis

The density functional theory (DFT) calculations at unrestricted B3LYP/6-31G(d,p) level was carried out using the quantum chemical package Gaussian 09W (15). The geometry of **3aa** was fully optimized in the gas phase and the empirical-dispersion correction was used during optimization.

3. Results and Discussion

3.1. Synthesis and Structural Analyses of the model GCDI 3aa

Initially, I intended to synthesize an amic acid-like structure with a β-carboxylic acid group (**Figure 1a**). Excess succinic anhydride was added to butylguanidine under basic conditions at ambient temperature. After a 24-h reaction, a hydrophobic compound was unexpectedly obtained as the major product, with an isolated yield of 85% at optimal conditions (**Table 1**). By ^{1}H-NMR and ^{13}C-NMR, it was confirmed that the compound was produced from one butylguanidine and two succinic anhydride molecules and that eight protons from the two succinic anhydride molecules exhibited only two singlet peaks (**Figure 5a**). Notably, the ^{13}C peak for the central carbon of the guanidine structure was observed at 128 ppm, abnormally upshifted by over 20 ppm compared to the peaks of other guanidine compounds (**Figure 5b**). COSY and HSQC analysis confirmed that the singlet peaks (**Figure 1b**, indicated as asterisks) were not coupled with each other and protons (in groups of four) were connected to structurally equivalent carbon atom(s) (**Figure 6**). The m/z ratio was measured as 280.2 ($[M+H]^{+}$) by liquid chromatography-mass spectroscopy (LC-MS), which confirmed the doubly dehydrated structure.

Finally, I obtained the single-crystal X-ray diffraction (SC-XRD) data of the compound, which showed a unique GCDI structure (**Figure 1c**). The crystal structure with two succinimide rings formed on different nitrogen atoms (N1 and N2) of guanidine was well-matched to the NMR and LC-MS data. The two rings appeared

to be in a skewed or *gauche* conformation, with a dihedral angle of 76°, suggesting disruption of the delocalized π-orbitals in the guanidine plane. The C9 - N3 bond (1.25 Å) was much shorter than that of arginine (1.35 Å), whereas the C9 - N1 (1.42 Å) and C9 - N2 (1.43 Å) bonds were significantly longer than those of arginine (1.32 - 1.34Å) (16, 17). The C9 - N3 bond showed a double bond character, but the other two C - N bonds exhibited single bond characters. The single-bond-like character permitted the rotation of the bonds such that the two succinimide rings exhibited a *gauche* conformation. The longer C - N bonds could rotate freely at room temperature, showing two singlet peaks of eight α-protons in two succinimide rings in the ^{1}H-NMR spectrum (**Figure 5a**). Density functional theory (DFT) calculations also predicted that the average positions of the two rings confirmed their *gauche* conformation in gas phase; the C1 - C4 ring was rather perpendicular to the C5 - C8 ring with a dihedral angle of 68° (**Figure 16**).

3.2. Syntheses of Various GCDI Structures

The scope of the cyclic anhydrides for the formation of other GCDI structures was investigated (**Figure 2**). Interestingly, the GCDI structure was not isolated by reaction with glutaric anhydride, a six-membered ring analog. On the other hand, other cyclic anhydrides with five-membered ring structures, such as *cis*-1,2-cyclohexanedicarboxylic anhydride (**2c**), phenylsuccinic anhydride (**2e**), and allylsuccinic anhydrides (**2f**), successfully produced GCDI products (**3ac**, **3ae**, and **3af**) in good yields of over 70%. Interestingly, the reaction with aromatic cyclic anhydrides such as phthalic anhydride (**2b**) and 4-bromo phthalic anhydride (**2d**) showed only moderate yields (30% - 50%). The results indicated that

GCDI formation was dependent upon the cyclization or dehydration between carboxylic acid and nitrogen (N1 or N2 in **Figure 1c**) of the guanidine-amic acid intermediate considering that the effective concentrations of the cyclization between nitrogen and carboxylic acid were significantly different in amic acid intermediates (18-22). Among the GCDI structures above, **3ae** and **3af** were obtained as mixtures of three stereoisomers with very similar hydrophobicity, as racemic mixtures of **2e** and **2f** were used for the reaction. GCDI formation was not confined to butylguanidine. A representative guanidine-possessing biomolecule, arginine, as a protected form, could also react with succinic anhydride to produce the expected GCDI structure **3ba** (**Figure 2**).

3.3. Degradation of GCDI Structures in Protic Solvents

Furthermore, I found that GCDI degraded much faster than imides in protic solvents. As shown in **Figure 17, 3aa** almost completely decomposed into butylguanidine (**1a**) after 48-h incubation at 37 °C in CD_3OD. **3aa** also hydrolyzed in D_2O and released butylguanidine and succinic acid, but the decomposition rate was much slower than that in CD_3OD (**Figure 18**). The addition of phosphate buffers accelerated the degradation in the pH range 3.1 - 9.6, and the degradation rate was fastest at pH = 9.6 (**Figure 20 - 23**). On the contrary, the compound was shown to be stable for weeks in aprotic solvents, *i.e.,* chloroform and dimethyl sulfoxide (**Figure 19 and 20**).

The formation and degradation of GCDI were much faster than those of amine-based imides under such mild conditions. The reactivity difference might be partially attributed to the acidity and basicity of the GCDI or intermediate structures. I proposed that GCDI

was formed from a guanidine-amic acid intermediate, which corresponded to the amic acid intermediate of amine-based imides (**Figure 27**). It was predicted that the acidity of the guanidine proton in the intermediate was far stronger than that of the amide proton due to the delocalization of the negative charge through the deprotonated guanidine structure, as confirmed by the higher acidity of many electron-withdrawing group-conjugated guanidines (23-27). Therefore, I expected that the nucleophilic attack by the deprotonated guanidine in the guanidine-amic acid intermediate on carboxylic acid for dehydration may be much more favorable than that by the amide in the formation of amine-based imides, facilitating GCDI formation under much milder conditions. In addition, protic solvents could attack the GCDI carbonyl group much more easily than the corresponding imides because the negative charge developed on nitrogen by the nucleophilic attack could be delocalized to the guanidine structure. Otherwise, unlike almost non-protonable imide correspondents, the alkylated nitrogen (N3 in **Figure 1c**) in the GCDI structure could be partially protonated under acidic conditions to accelerate the nucleophilic attack of solvent molecules by enhancing the electrophilicity of the imide carbonyl group (**Figure 28**).

4. Conclusion

In summary, I first report that GCDI structures can be formed from guanidine-based molecules and five-membered ring cyclic anhydrides under very mild conditions. The two diimide rings are in *gauche* conformation, as confirmed by NMR and SC-XRD. The allene-like *gauche* conformation could be an excellent structural center for the synthesis of unreported molecules. GCDI is quite stable in aprotic solvents, but readily degrades in protic solvents, probably because of the charge-delocalized guanidine structure. The unique reactive characteristics of the obtained GCDI structure are very attractive for the synthesis of imide-like structures under mild conditions or for the development of smart degradable materials in biologically-tolerable conditions.

References

(1) McLeish, M. J.; Kenyon, G. L. *Crit. Rev. Biochem. Mol. Biol.* **2005**, *40*, 1-20.

(2) Chau, J.; Ciufolini, M. A. *Mar. Drugs* **2011**, *9*, 2046-2074.

(3) Cragoe, E. J.; Woltersdorf, O. W.; Bicking, J. B.; Kwong, S. F.; Jones, J. H. *J. Med. Chem.* **1967**, *10*, 66-75.

(4) Watanabe, M.; Koike, H.; Ishiba, T.; Okada, T.; Seo, S.; Hirai, K. *Bioorg. Med. Chem.* **1997**, *5*, 437-444.

(5) Fuhrmann, J.; Schmidt, A.; Spiess, S.; Lehner, A.; Turgay, K.; Mechtler, K.; Charpentier, E.; Clausen, T. *Science* **2009**, *324*, 1323-1327.

(6) Grundler, V.; Gademann, K. *ACS Med. Chem. Lett.* **2014**, *5*, 1290-1295.

(7) Keller, M.; Pop, N.; Hutzler, C.; Beck-Sickinger, A. G.; Bernhardt, G.; Buschauer, A. *J. Med. Chem.* **2008**, *51*, 8168-8172.

(8) Gálvez, A. O.; Schaack, C. P.; Noda, H.; Bode, J. W. *J. Am. Chem. Soc.* **2017**, *139*, 1826-1829.

(9) Kühle, E.; Anders, B.; Zumach, G. *Angew. Chem.* **1967**, *79*, 663-680.

(10) Gund, P. *J. Chem. Educ.* **1972**, *49*, 100-103.

(11) Kavitha, K.; Praveena, K. S. S.; Ramarao, E. V. V. S.; Murthy, N. Y. S.; Pal, S. *Curr. Org. Chem.* **2016**, *20*, 1955-2001.

(12) Patil, M. M.; Rajput, S. S. *Int. J. Pharm. Pharm. Sci.* **2014**, *6*, 8-14.

(13) *APEX2*, version 2009.1; Data collection and Processing software; Bruker AXS Inc.: Madison, WI, 2008.

(14) *SHELXTL-PC*, version 6.14; Program for solution and refinement of crystal structure; Bruker AXS Inc.: Madison, WI, 2001.

(15) Frisch, M. J.; Trucks, G. W.; Schlegel, H. B.; Scuseria, G. E.; Robb, M. A.; Cheeseman, J. R.; Scalmani, G.; Barone, V.; Mennucci, B.; Petersson, G. A.; Nakatsuji, H.; Caricato, M.; Li, X.; Hratchian, H. P.; Izmaylov, A. F.; Bloino, J.; Zheng, G.; Sonnenberg, J. L.; Hada, M.; Ehara, M.; Toyota, K.; Fukuda, R.; Hasegawa, J.; Ishida, M.; Nakajima, T.; Honda, Y.; Kitao, O.; Nakai, H.; Vreven, T.; Montgomery, J. A., Jr.; Peralta, J. E.; Ogliaro, F.; Bearpark, M. J.; Heyd, J.; Brothers, E. N.; Kudin, K. N.; Staroverov, V. N.; Kobayashi, R.; Normand, J.; Raghavachari, K.; Rendell, A. P.; Burant, J. C.; Iyengar, S. S.; Tomasi, J.; Cossi, M.; Rega, N.; Millam, N. J.; Klene, M.; Knox, J. E.; Cross, J. B.; Bakken, V.; Adamo, C.; Jaramillo, J.; Gomperts, R.; Stratmann, R. E.; Yazyev, O.; Austin, A. J.; Cammi, R.; Pomelli, C.; Ochterski, J. W.; Martin, R. L.; Morokuma, K.; Zakrzewski, V. G.; Voth, G. A.; Salvador, P.; Dannenberg, J. J.; Dapprich, S.; Daniels, A. D.; Farkas, Ö.; Foresman, J. B.; Ortiz, J. V.; Cioslowski, J.; Fox, D. J. *Gaussian 09*; Gaussian, Inc.: Wallingford, CT, 2009.

(16) Lehmann, M. S.; Verbist, J. J.; Hamilton, W. C.; Koetzle, T. F. *J. Chem. Soc., Perkin Trans. 2* **1973**, 133-137.

(17) Kingsford-Adaboh, R.; Grosche, M.; Dittrich, B.; Luger, P. *Acta Crystallogr., Sect. C: Cryst. Struct. Commun.* **2000**, *56*, 1274-1276.

(18) Kirby, A.J. *Adv. Phys. Org. Chem.* **1980**, *17*, 183-278.

(19) Haddadin, M. J.; Higuchi, T.; Stella, V. *J. Pharm. Sci.* **1975**, *64*, 1759-1765.

(20) Bruice, T. C.; Pandit, U. K. *J. Am. Chem. Soc.* **1960**, *82*, 5858-5865.

(21) Gaetjens, E.; Morawetz, H. *J. Am. Chem. Soc.* **1960**, *82*, 5328-5335.

(22) Bruice, T. C.; Pandit, U. K. *Proc. Natl. Acad. Sci. U.S.A.* **1960**,

46, 402-404.
(23) Ko, S. Y.; Lerpiniere, J.; Christofi, A. M. *Synlett.* **1995**, 815-816.
(24) Vaidyanathan, G.; Zalutsky, M. R. *J. Org. Chem.* **1997**, *62*, 4867-4869.
(25) Miyabe, H.; Yoshida, K.; Reddy, V. K.; Takemoto, Y. *J. Org. Chem.* **2009**, *74*. 305-311.
(26) Powell, D. A.; Ramsden, P. D.; Batey, R. A. *J. Org. Chem.* **2003**, *68*, 2300-2309.
(27) Miyabe, H.; Matsumura, A.; Yoshida, K.; Yamauchi, M.; Takemoto, Y. *Lett. Org. Chem.* **2004**, *1*, 119-121.

Figures

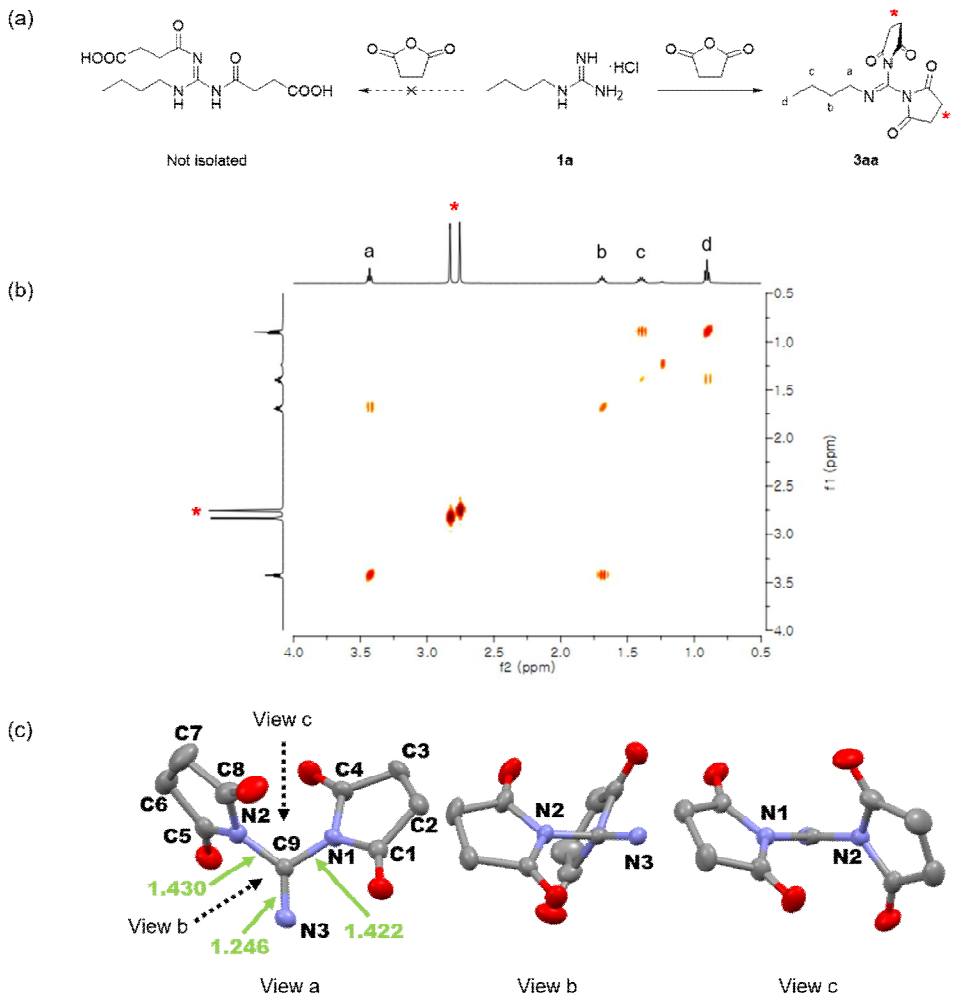

Figure 1. Synthesis and structure of guanidine cyclic diimide (GCDI). (a) Synthesis scheme, (b) COSY NMR spectrum and (c) X-ray crystal structure of GCDI molecule (**3aa**). ^{1}H-NMR peaks of succinimide rings are indicated as asterisks in the COSY spectrum. Butyl group and all hydrogen atoms are omitted in the crystal structure for clarity. The C - N bond lengths (Å) are indicated in green.

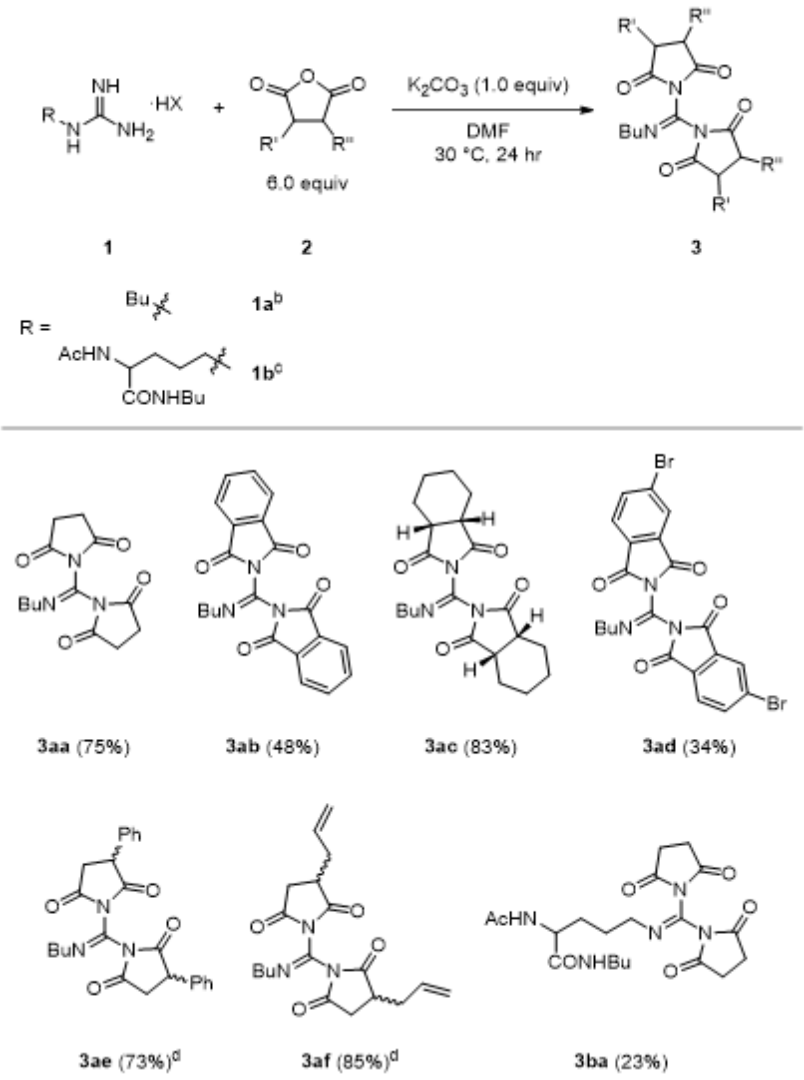

[a]Isolated yields. [b]Used as hydrochloride salt. [c]Used as trifluoroacetate salt. [d]Isolated as a mixture of diastereomers.

Figure 2. GCDI structures from various cyclic anhydrides[a]

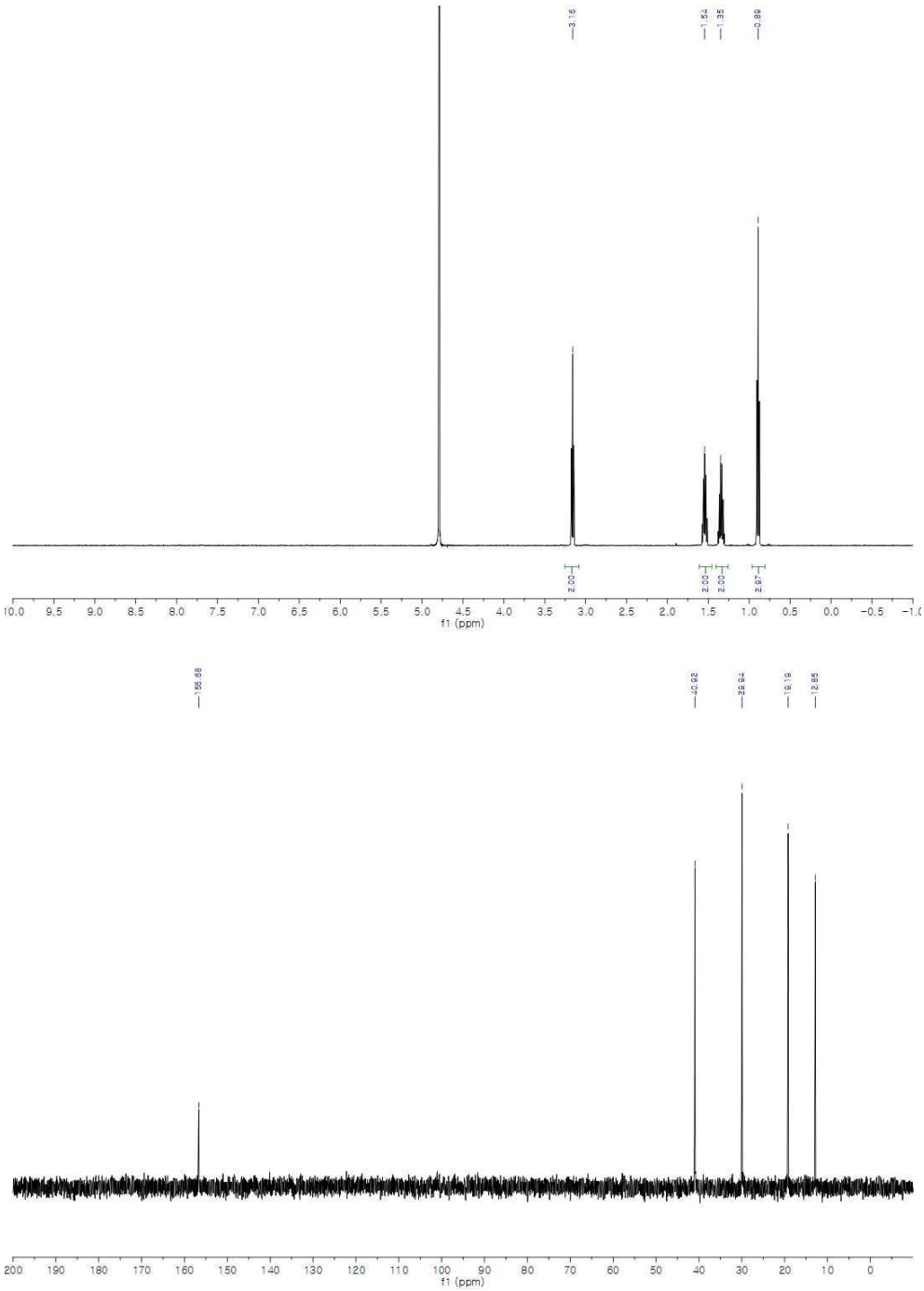

Figure 3. (a) ^{1}H- and (b) ^{13}C-NMR of compound **1a** in D_2O

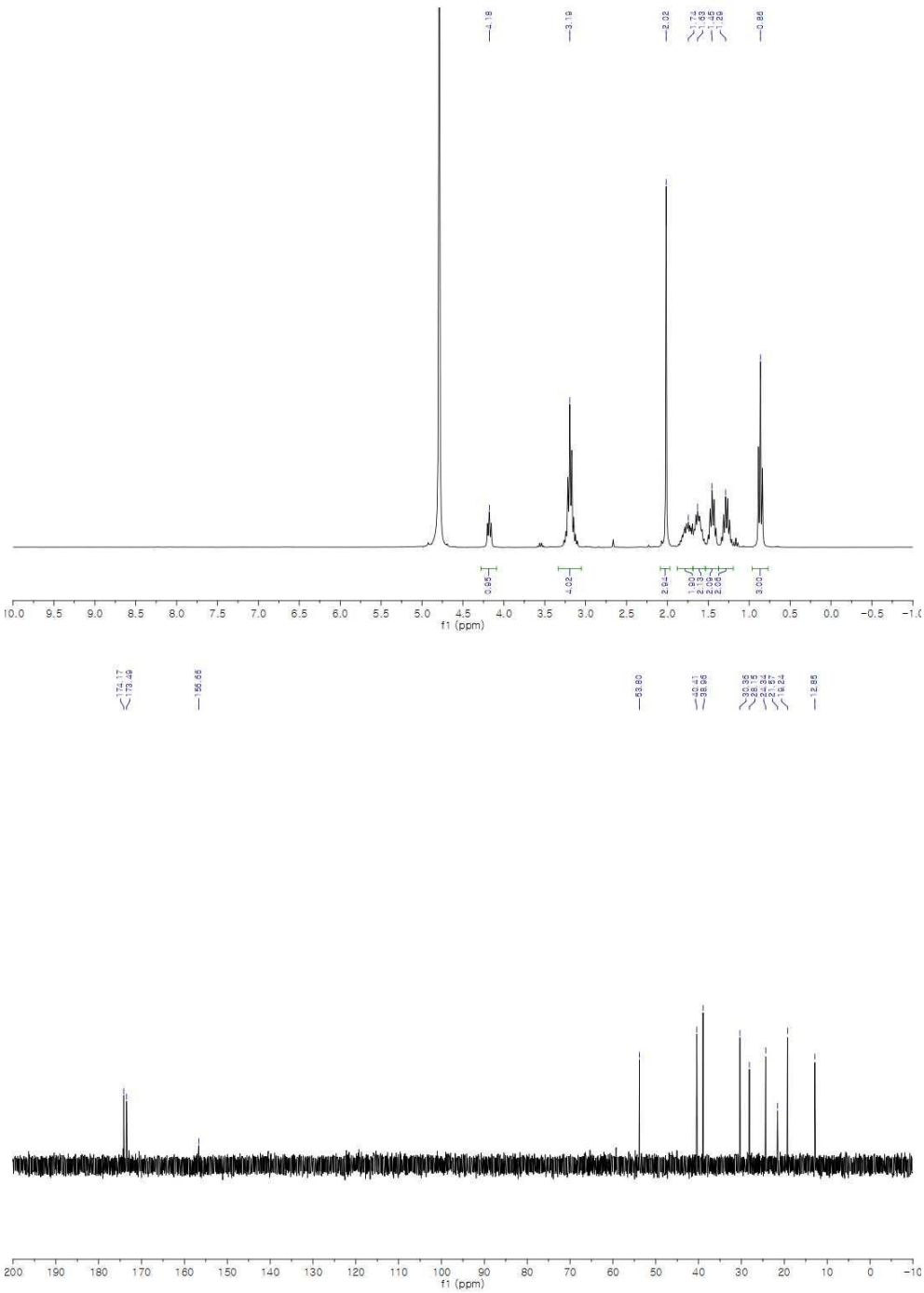

Figure 4. (a) ^{1}H- and (b) ^{13}C-NMR of compound **1b** in D_2O

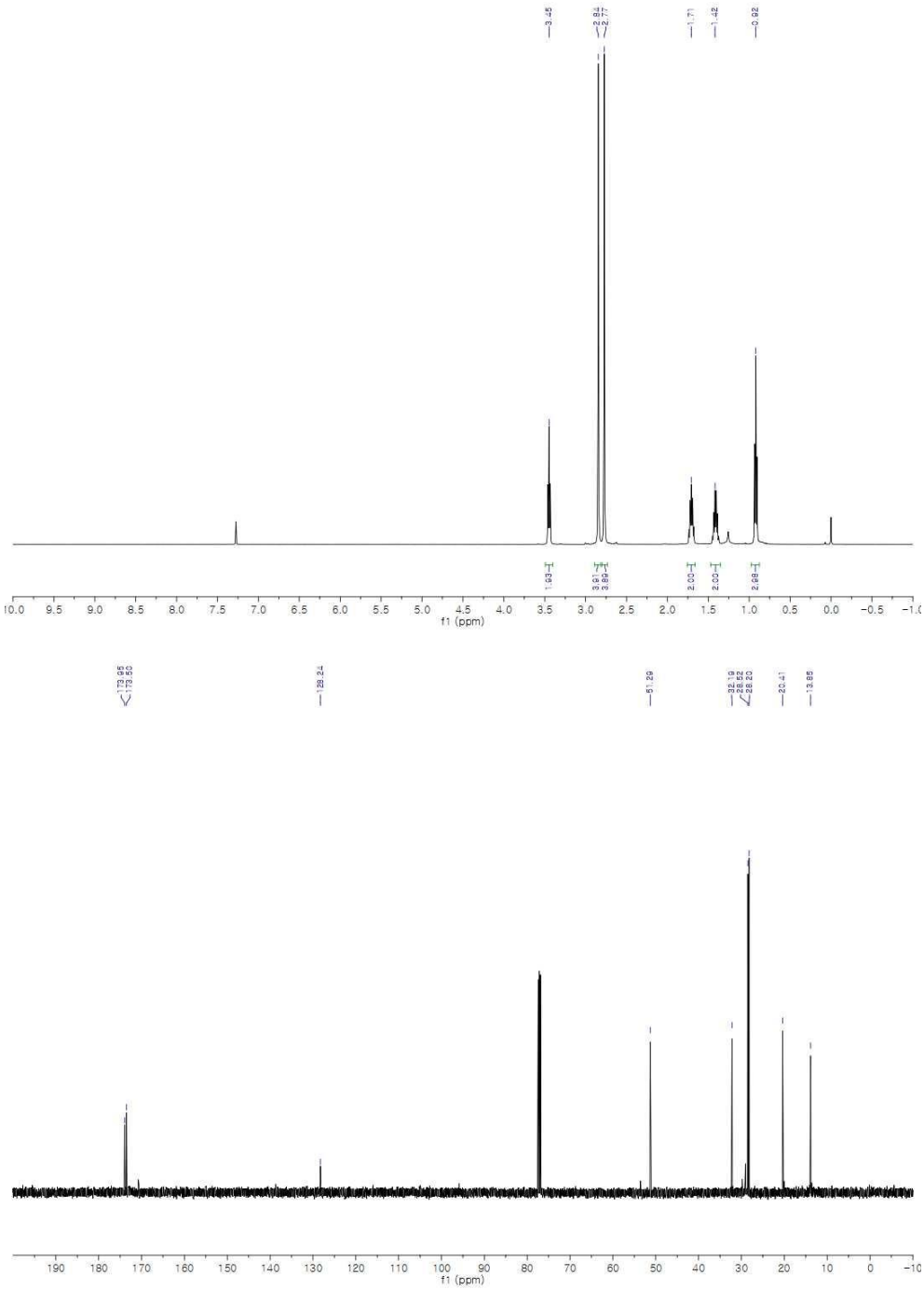

Figure 5. (a) ^{1}H- and (b) ^{13}C-NMR of compound **3aa** in $CDCl_3$

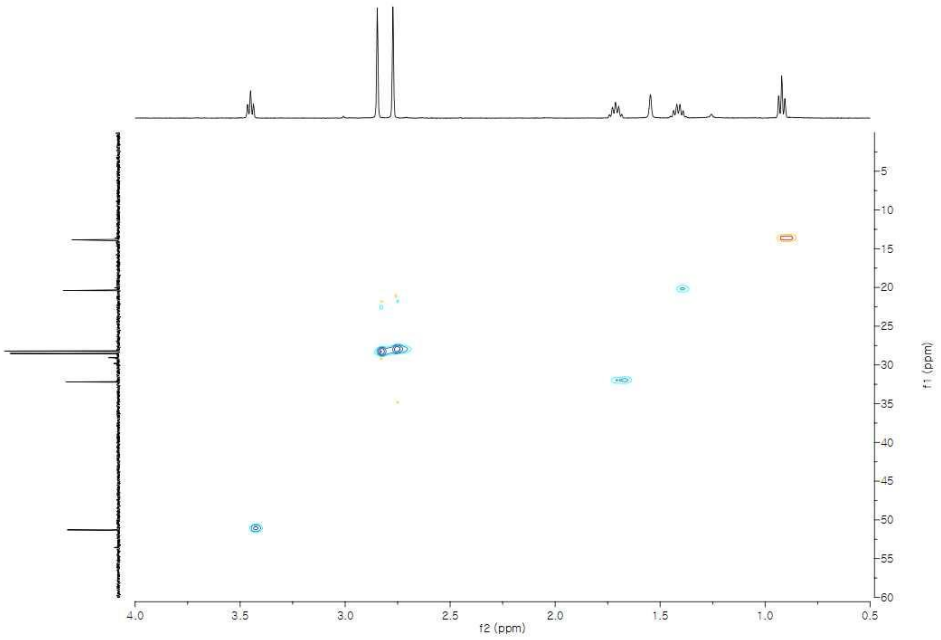

Figure 6. HSQC spectrum of compound **3aa** in $CDCl_3$

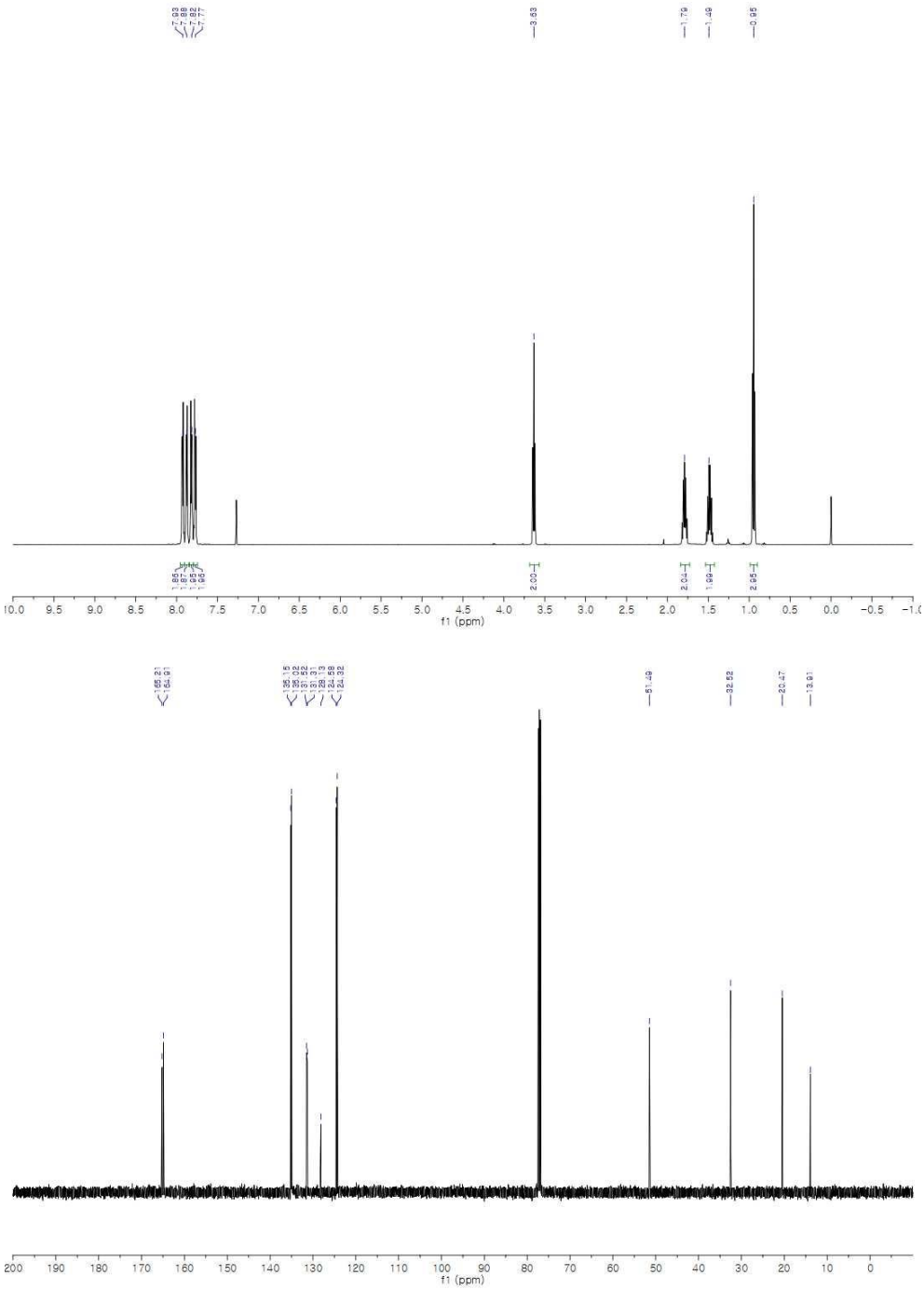

Figure 7. (a) ^{1}H- and (b) ^{13}C-NMR of compound **3ab** in $CDCl_3$

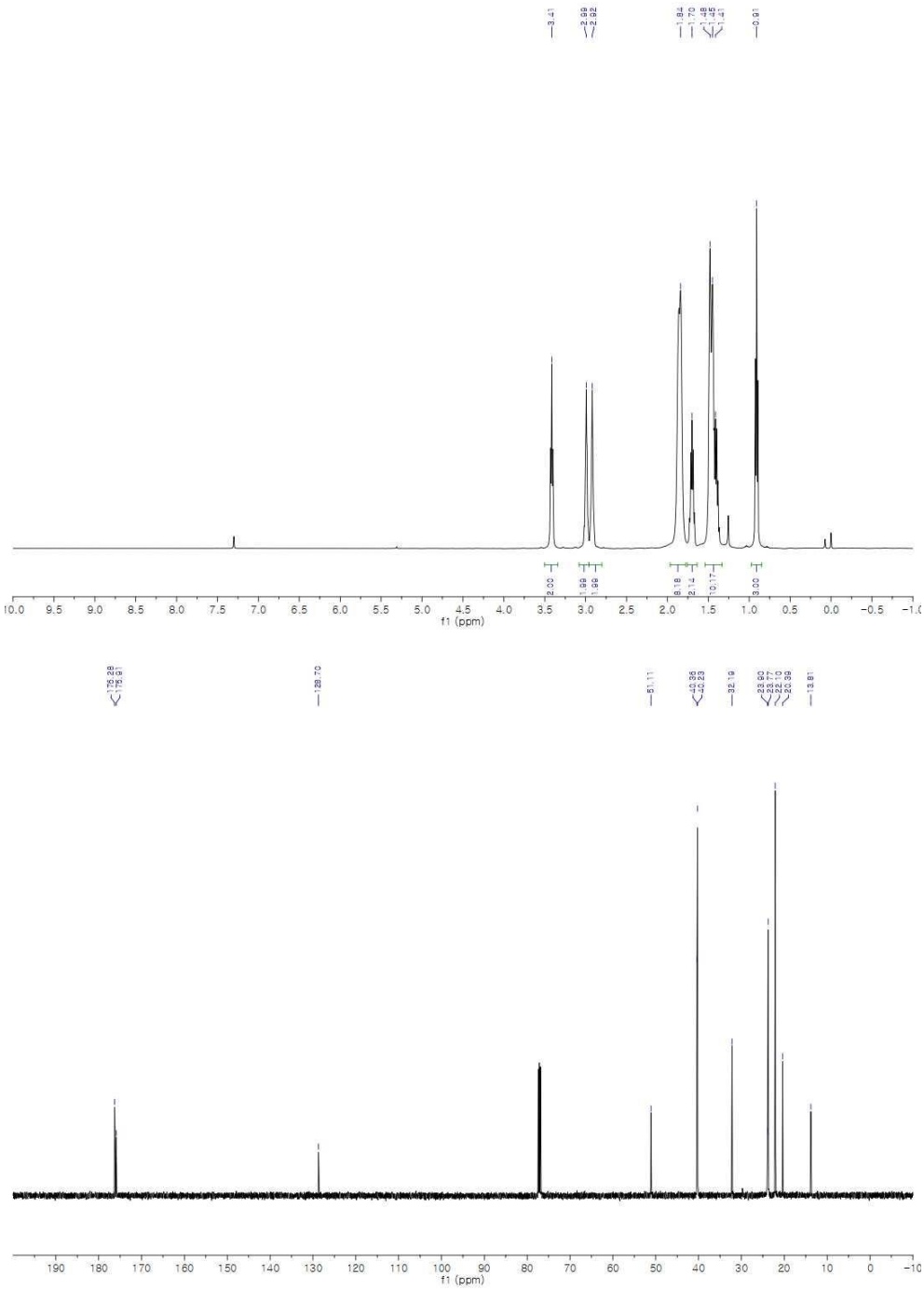

Figure 8. (a) ^{1}H- and (b) ^{13}C-NMR of compound **3ac** in $CDCl_3$

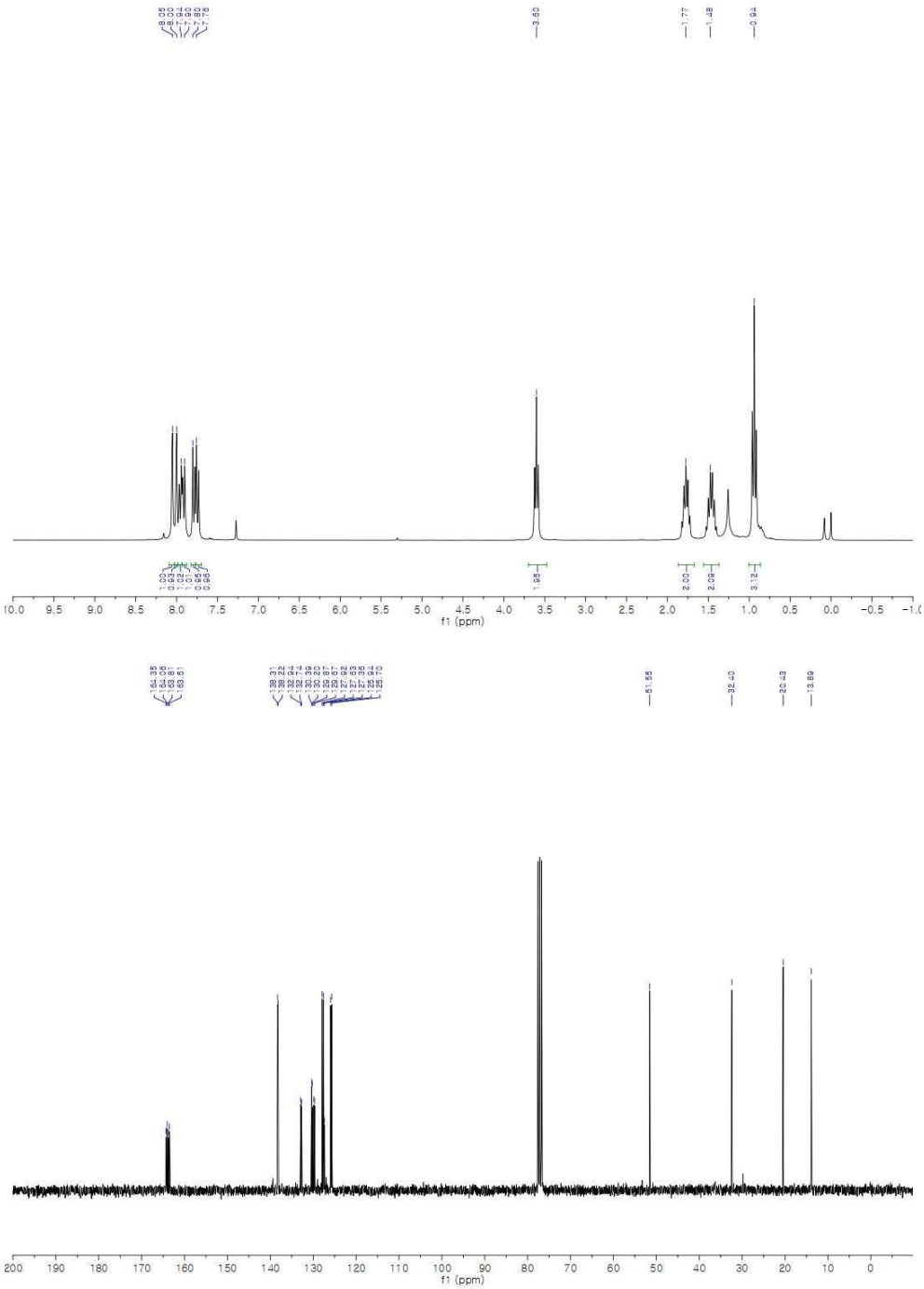

Figure 9. (a) ^{1}H- and (b) ^{13}C-NMR of compound **3ad** in $CDCl_3$

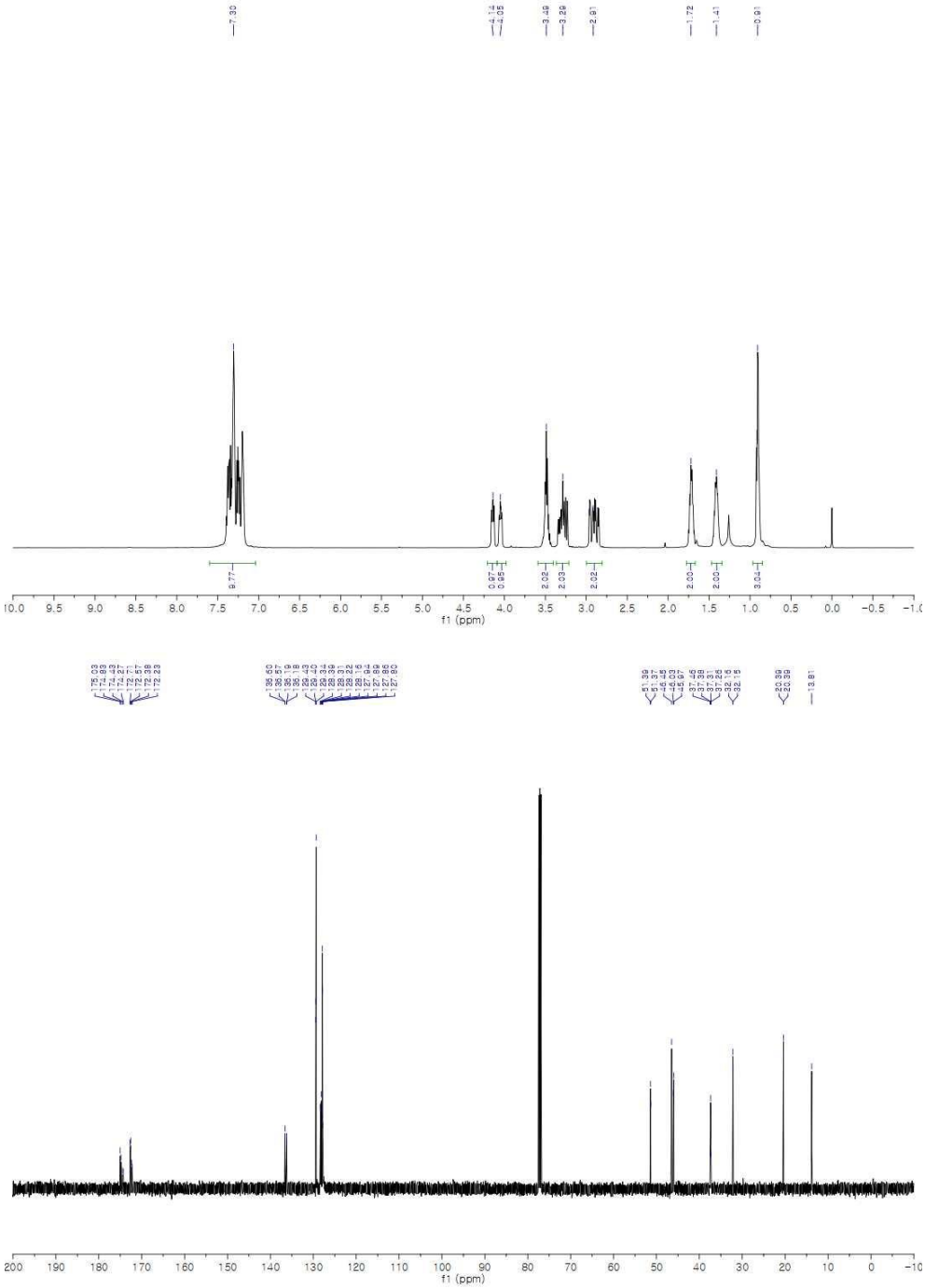

Figure 10. (a) ^{1}H- and (b) ^{13}C-NMR of compound **3ae** in $CDCl_3$

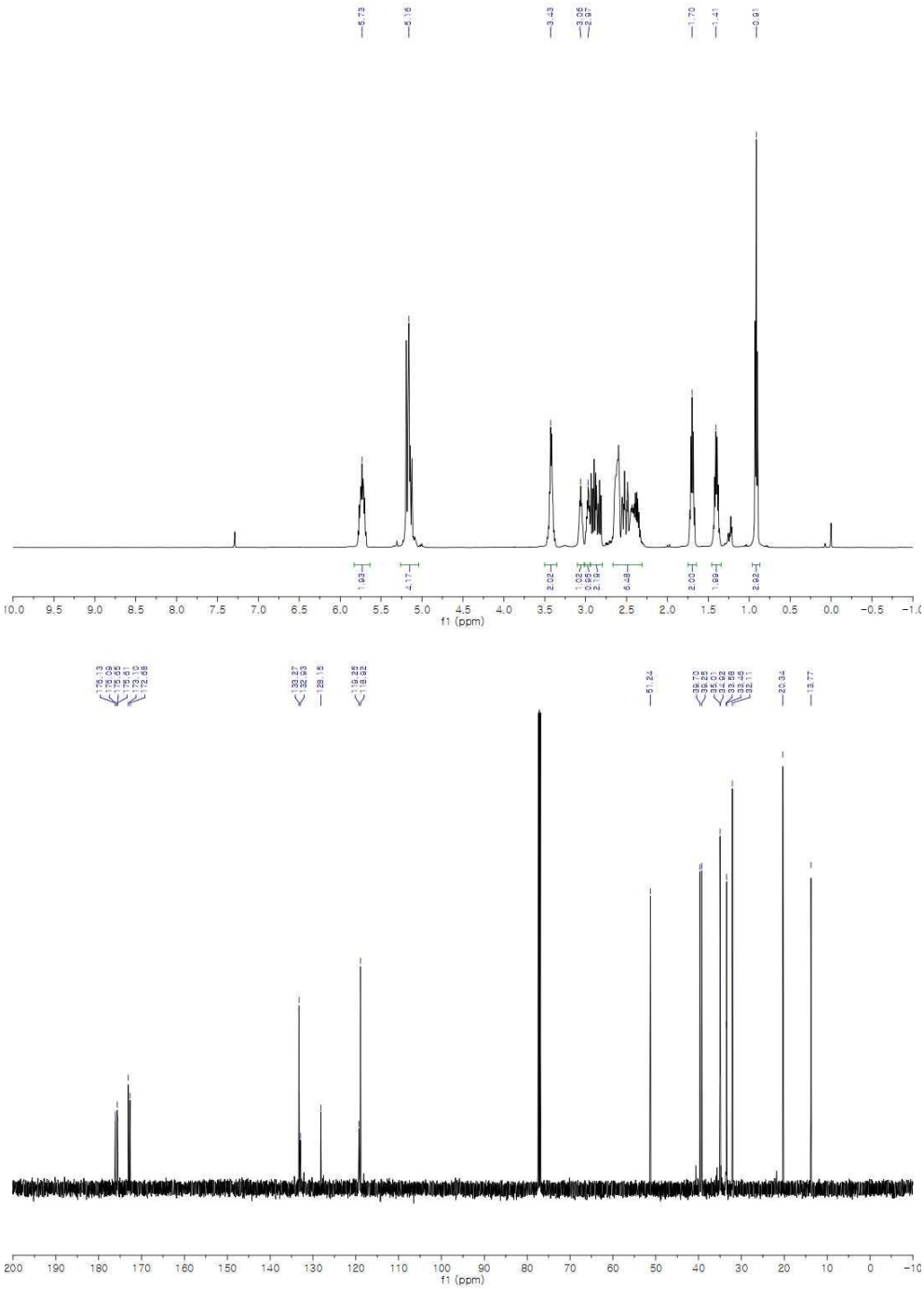

Figure 11. (a) ^{1}H- and (b) ^{13}C-NMR of compound **3af** in $CDCl_3$

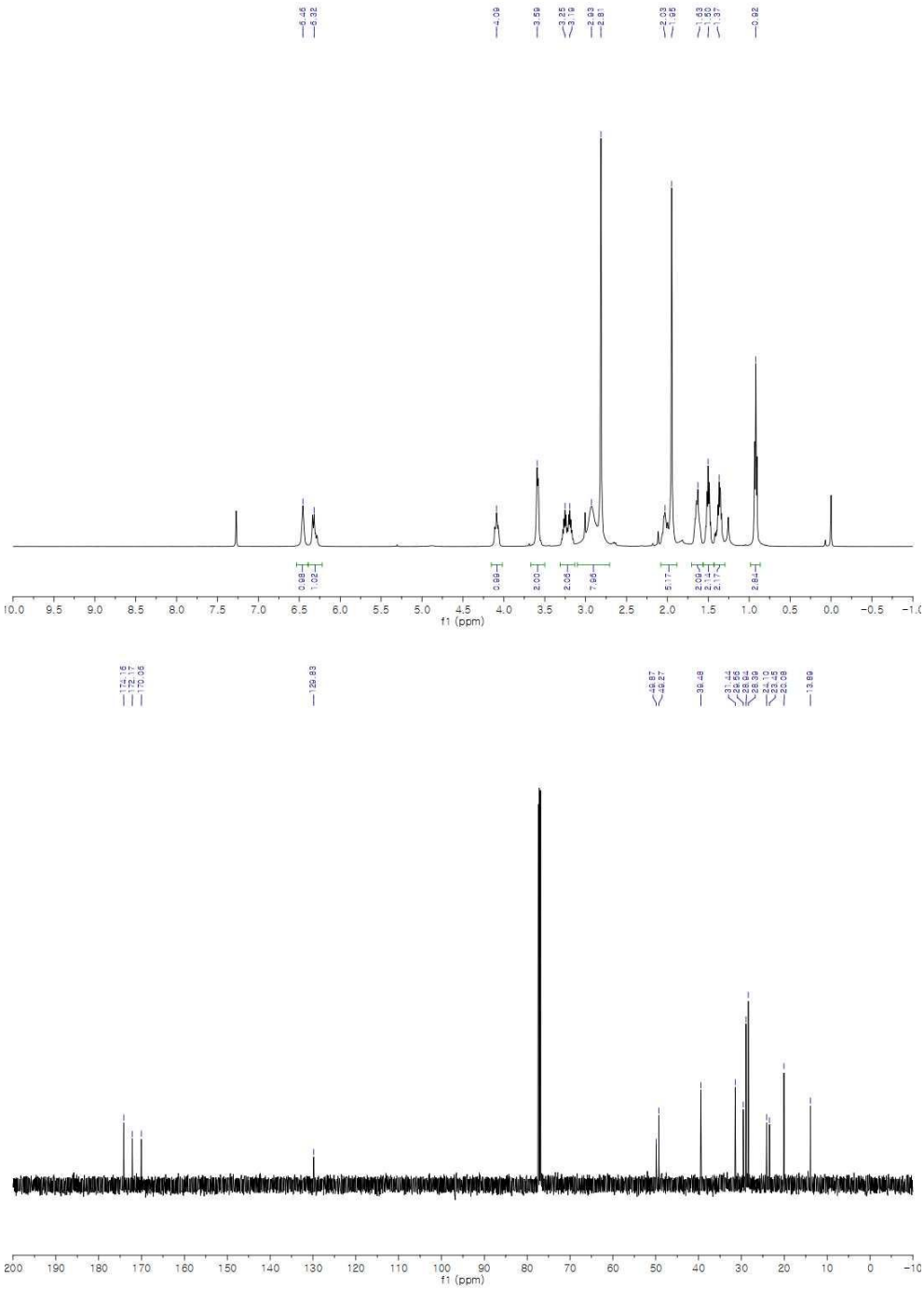

Figure 12. (a) ^{1}H- and (b) ^{13}C-NMR of compound **3ba** in $CDCl_3$

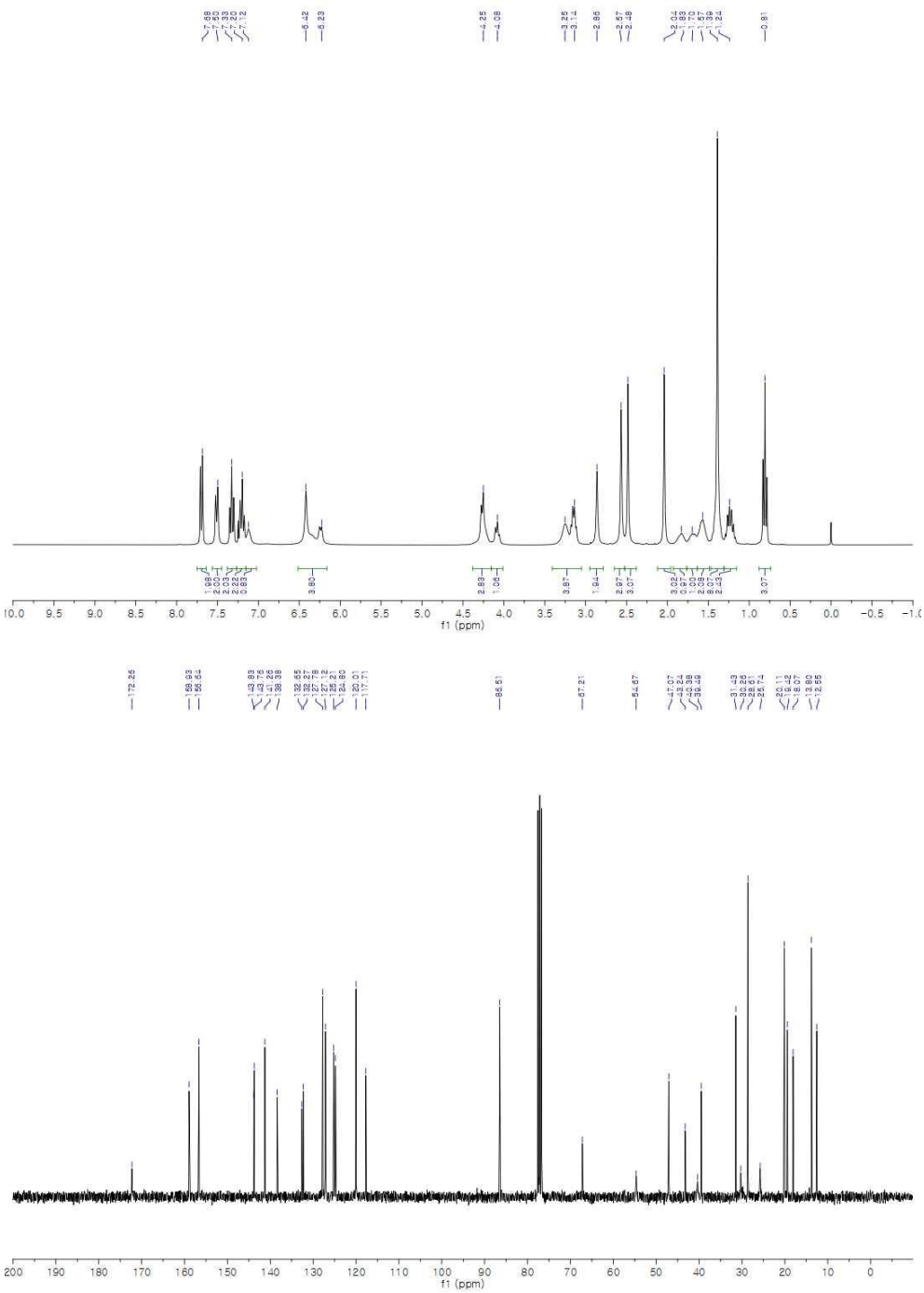

Figure 13. (a) ^{1}H- and (b) ^{13}C-NMR of compound **4** in $CDCl_3$

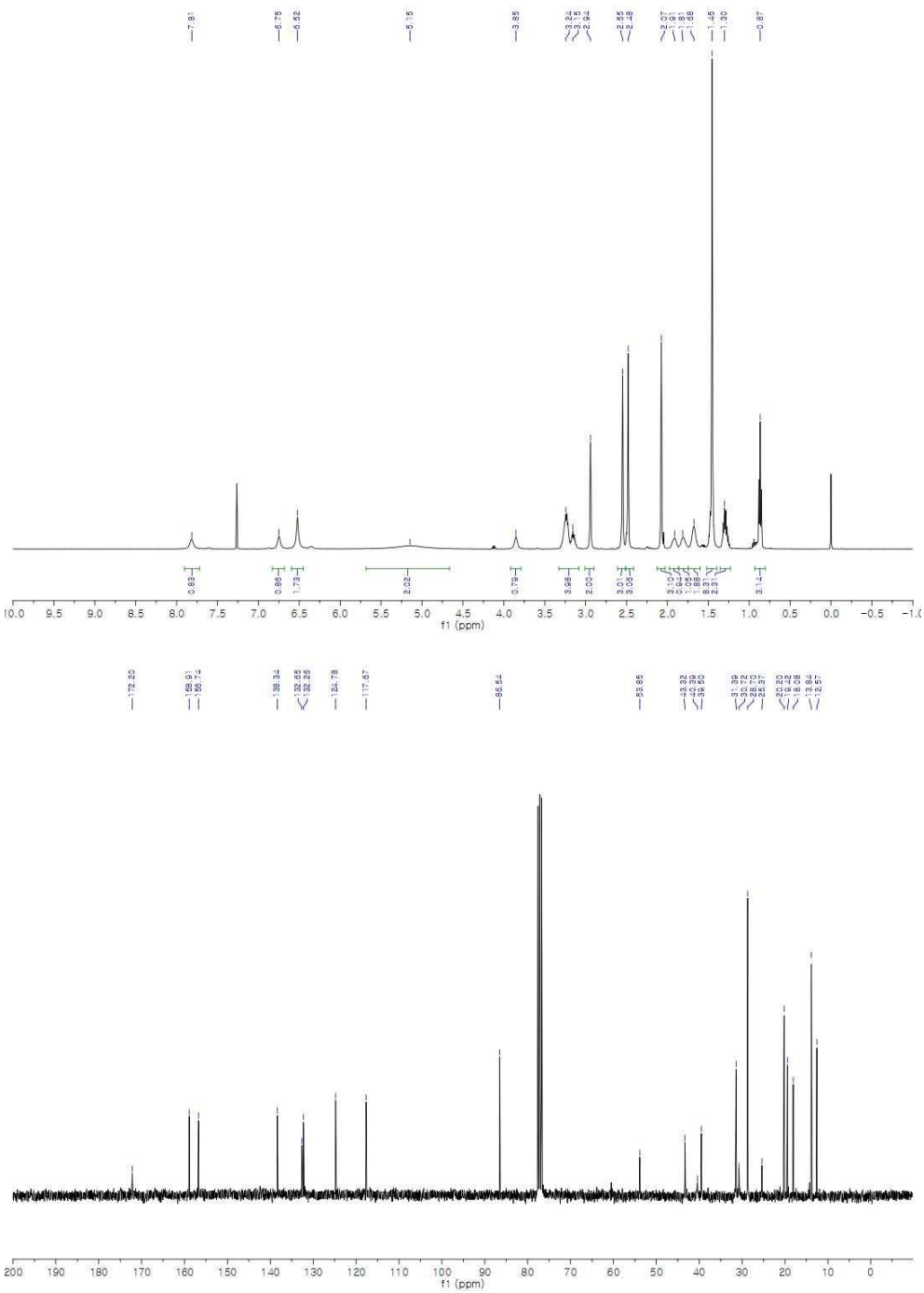

Figure 14. (a) ^{1}H- and (b) ^{13}C-NMR of compound **5** in $CDCl_3$

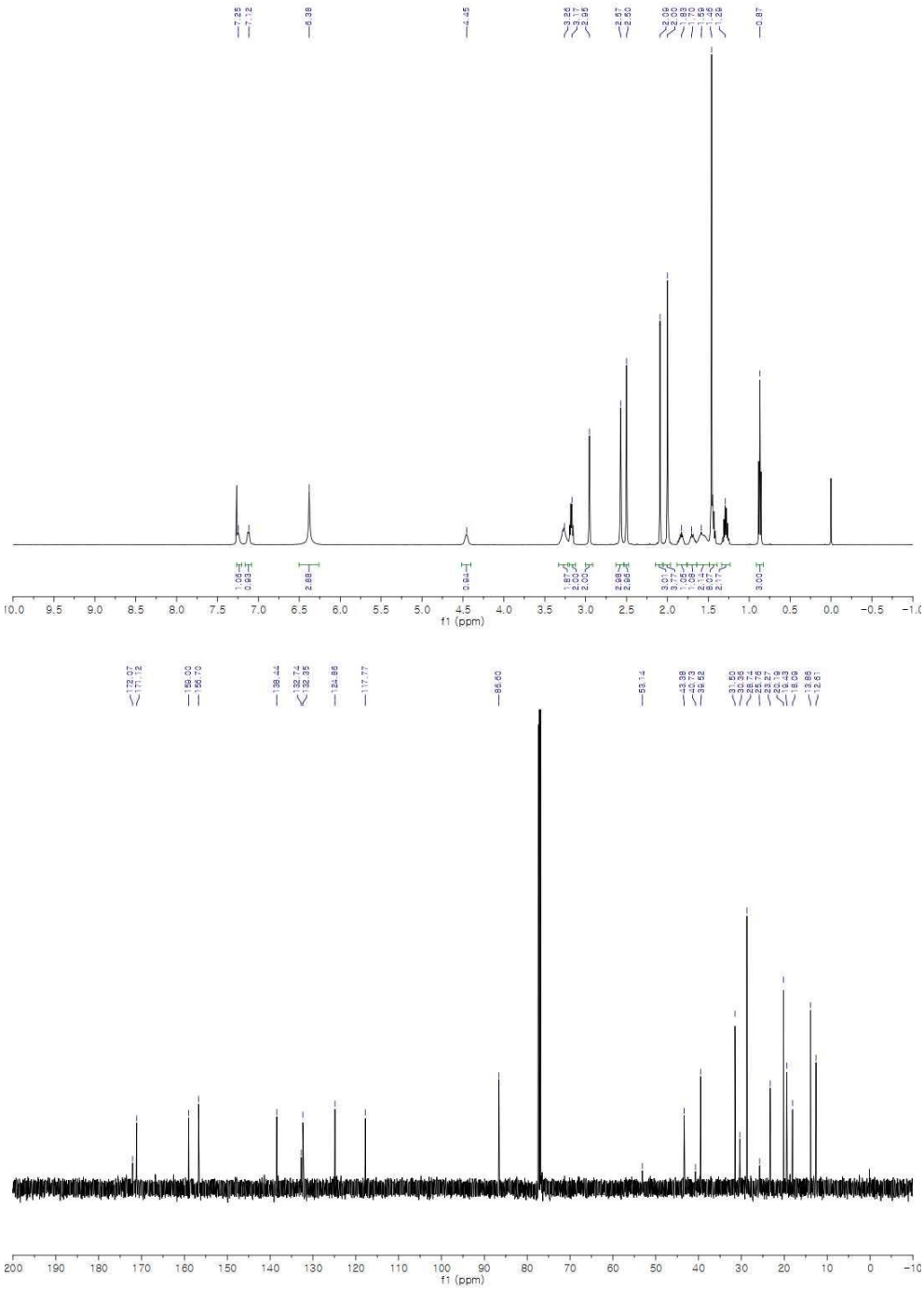

Figure 15. (a) ^{1}H- and (b) ^{13}C-NMR of compound **6** in $CDCl_3$

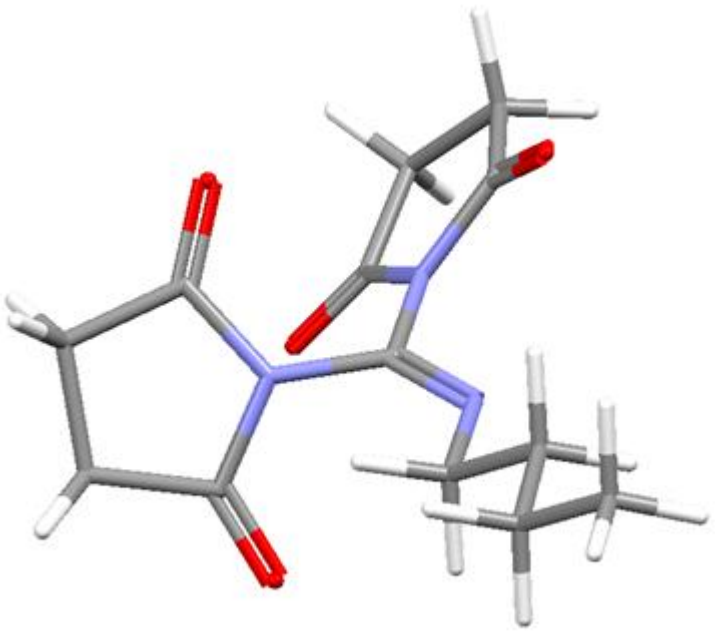

Figure 16. DFT-optimized molecular structure of **3aa**

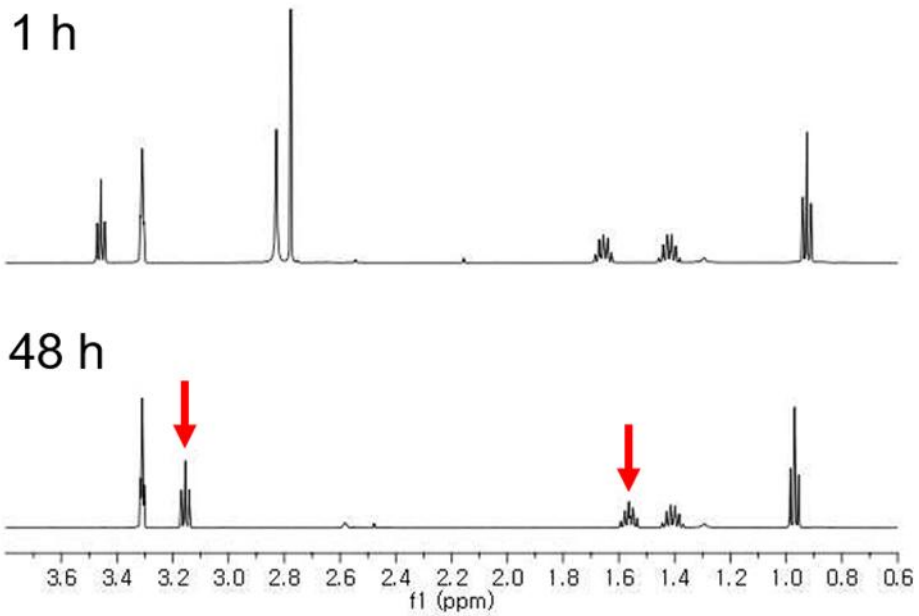

Figure 17. Degradation of **3aa** and release of butylguanidine (red arrow) in CD_3OD at 37 °C traced by ^1H-NMR.

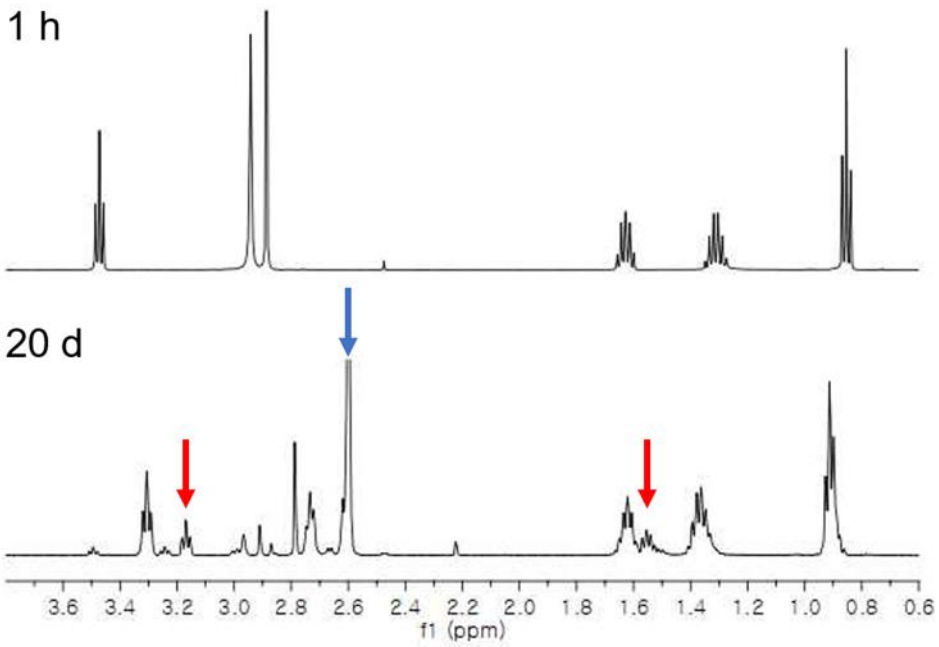

Figure 18. 3aa was incubated in D_2O (5 mg/ml, 37 °C) and ^1H-NMR spectra were recorded on Varian NMR System 500 MHz. After incubation for 20 days, release of butylguanidine (red arrow) and succinic acid (blue arrow) was observed.

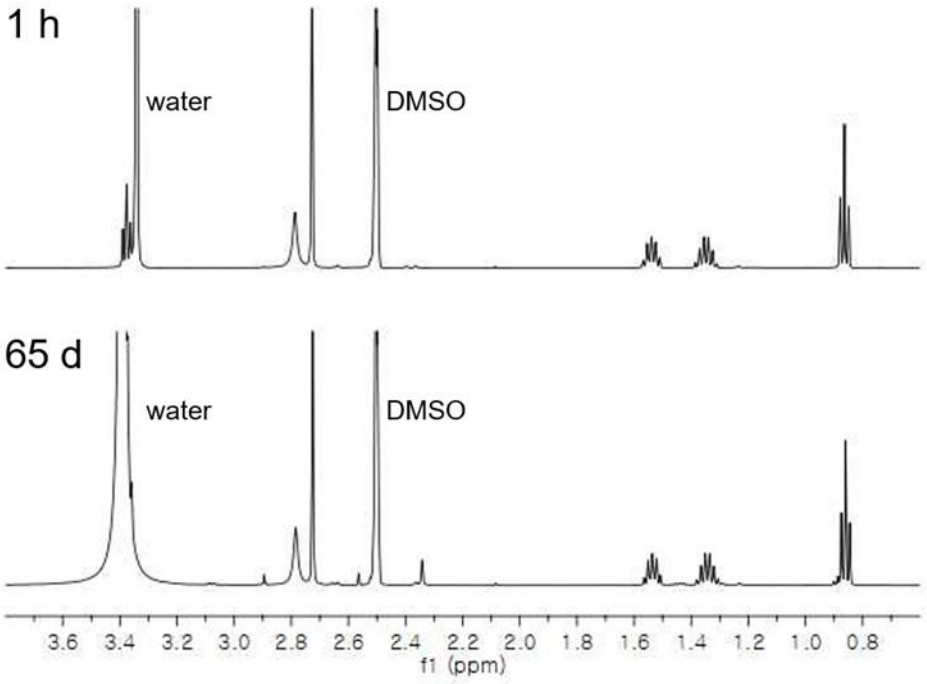

Figure 19. 3aa was incubated in d^6-DMSO (5 mg/ml, 37 °C) and ^{1}H-NMR spectra were recorded on Varian NMR System 500 MHz. No significant change in ^{1}H-NMR spectrum was observed after incubation for 65 days.

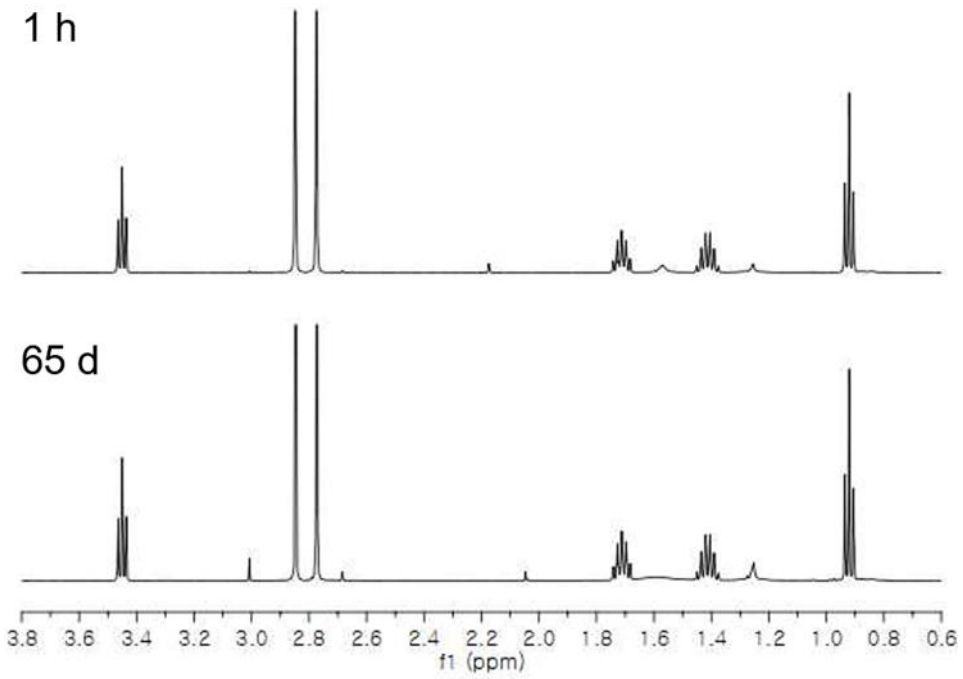

Figure 20. 3aa was incubated in $CDCl_3$ (5 mg/ml, 37 °C) and ^{1}H-NMR spectra were recorded on Varian NMR System 500 MHz. No significant change in ^{1}H-NMR spectrum was observed after incubation for 65 days.

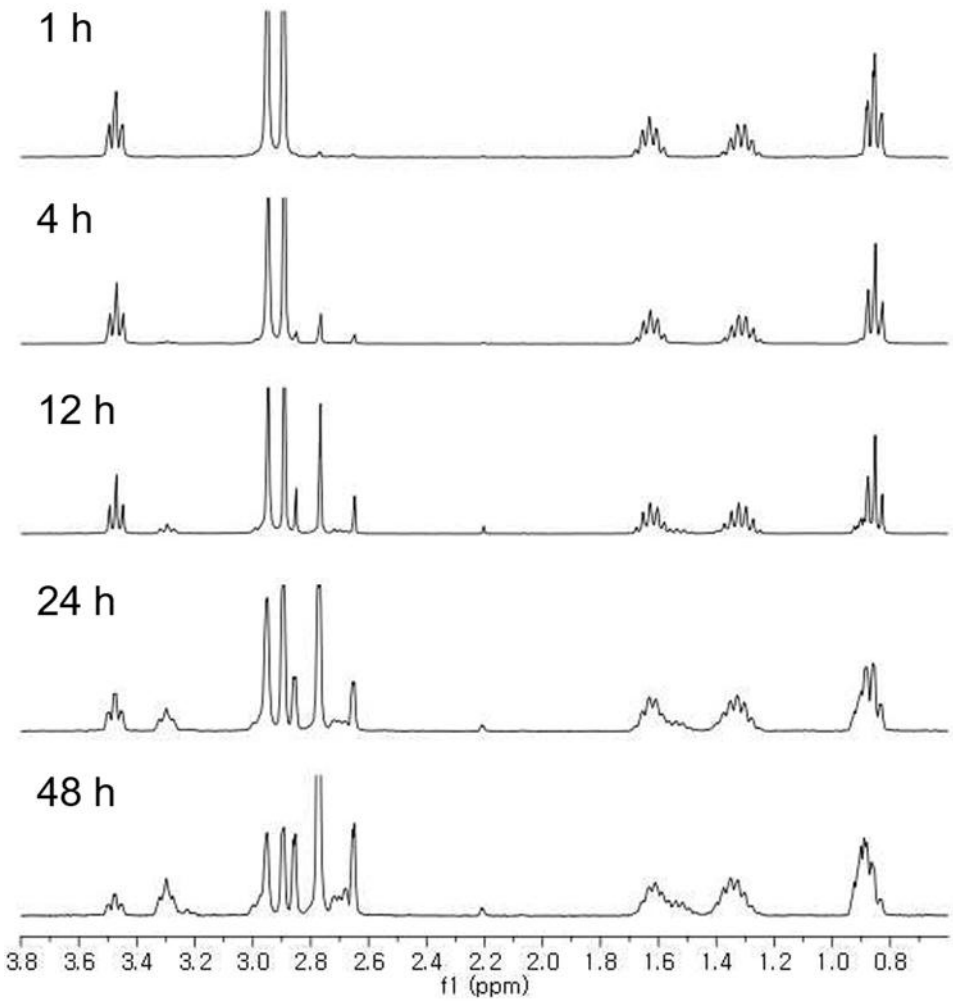

Figure 21. 3aa was incubated in 250 mM deuterated phosphate buffer (pD 3.1, 5 mg/ml, 37 °C) and ^{1}H-NMR spectra were recorded on Bruker Avance DPX-300.

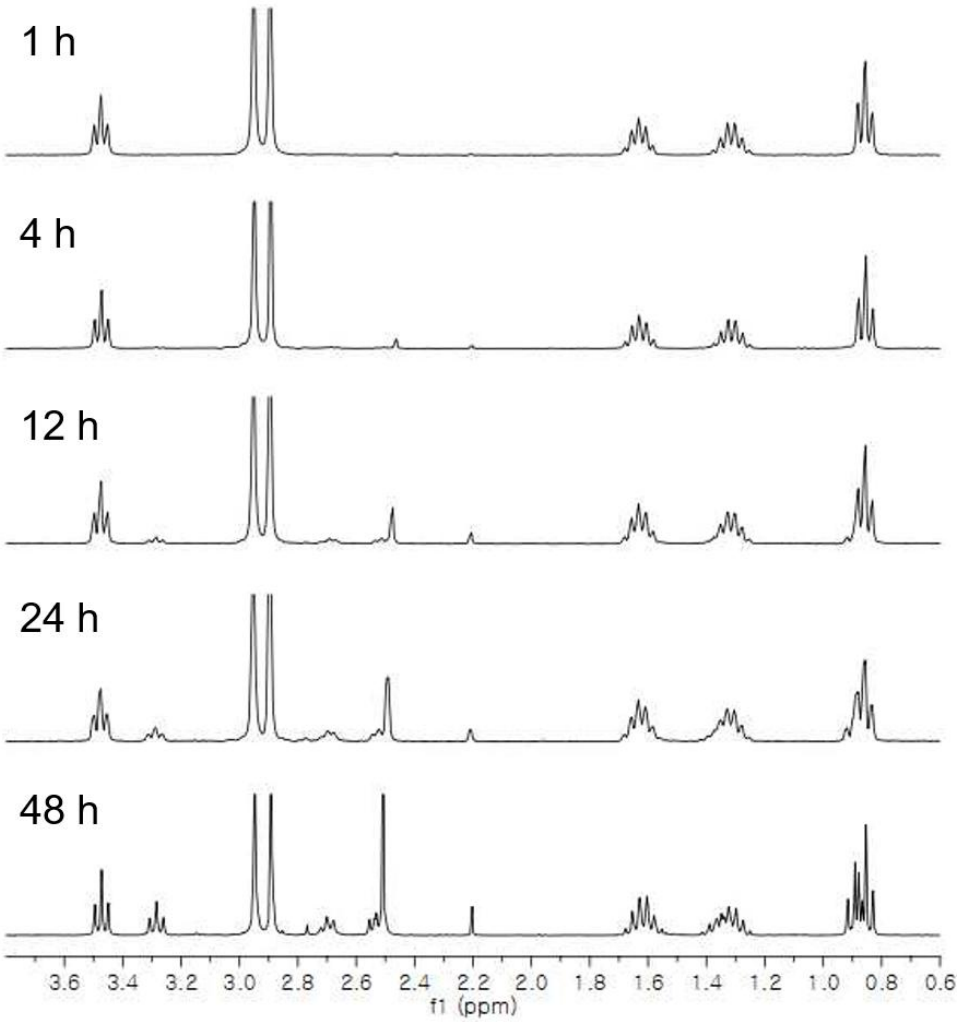

Figure 22. 3aa was incubated in 250 mM deuterated phosphate buffer (pD 5.5, 5 mg/ml, 37 °C) and ^{1}H-NMR spectra were recorded on Bruker Avance DPX-300.

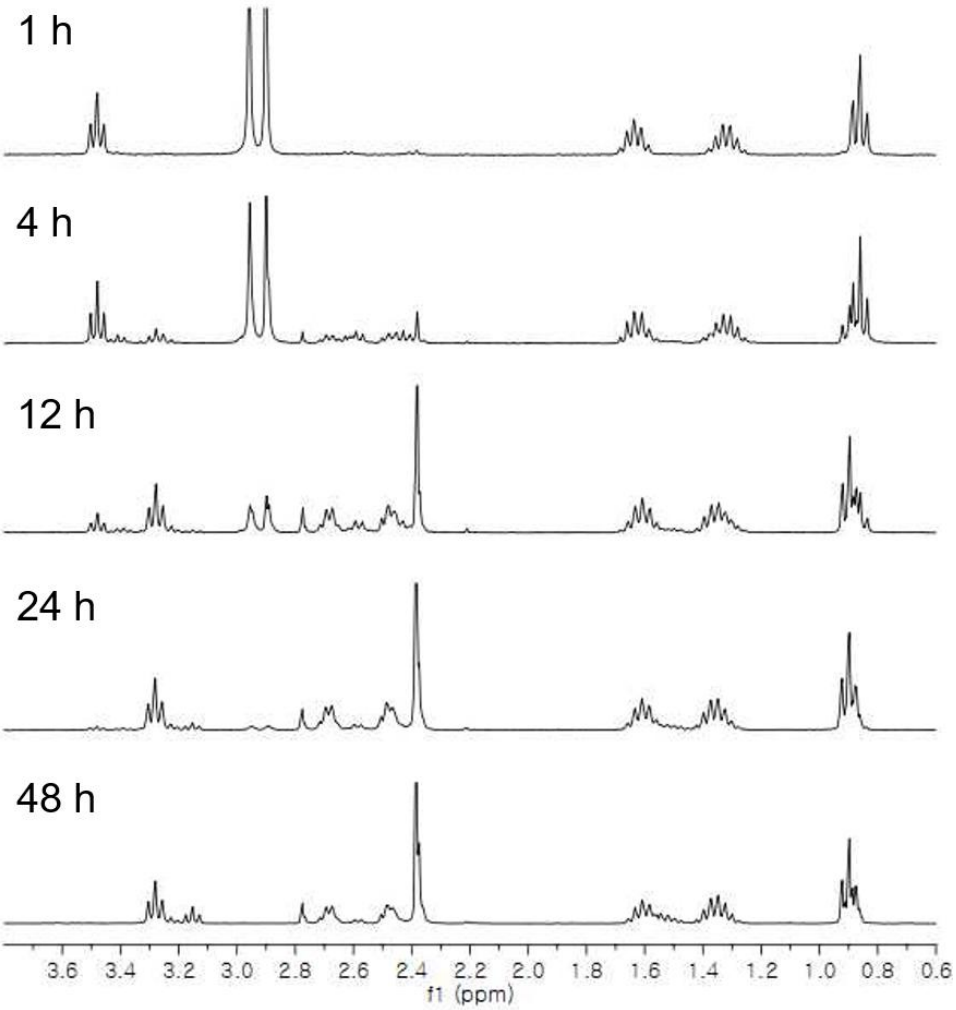

Figure 23. 3aa was incubated in 250 mM deuterated phosphate buffer (pD 7.5, 5 mg/ml, 37 °C) and ^{1}H-NMR spectra were recorded on Bruker Avance DPX-300.

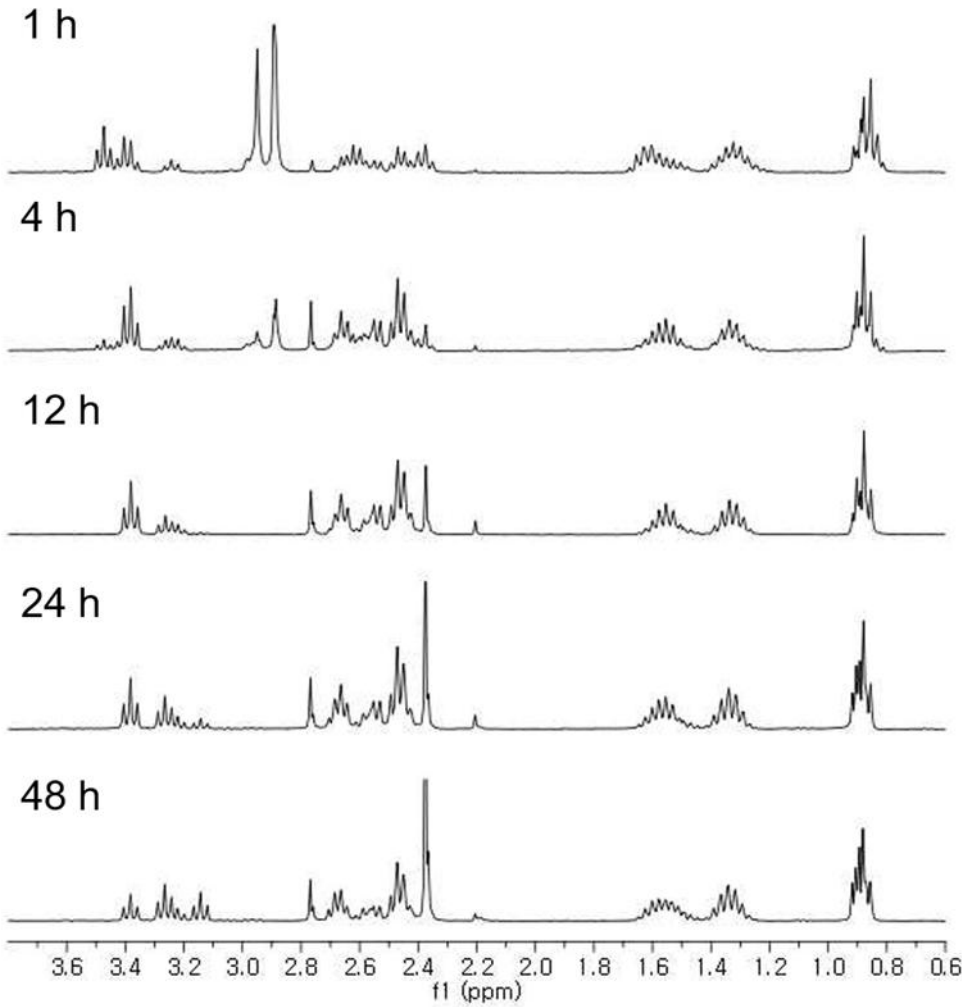

Figure 24. 3aa was incubated in 250 mM deuterated phosphate buffer (pD 9.6, 5 mg/ml, 37 °C) and ^{1}H-NMR spectra were recorded on Bruker Avance DPX-300.

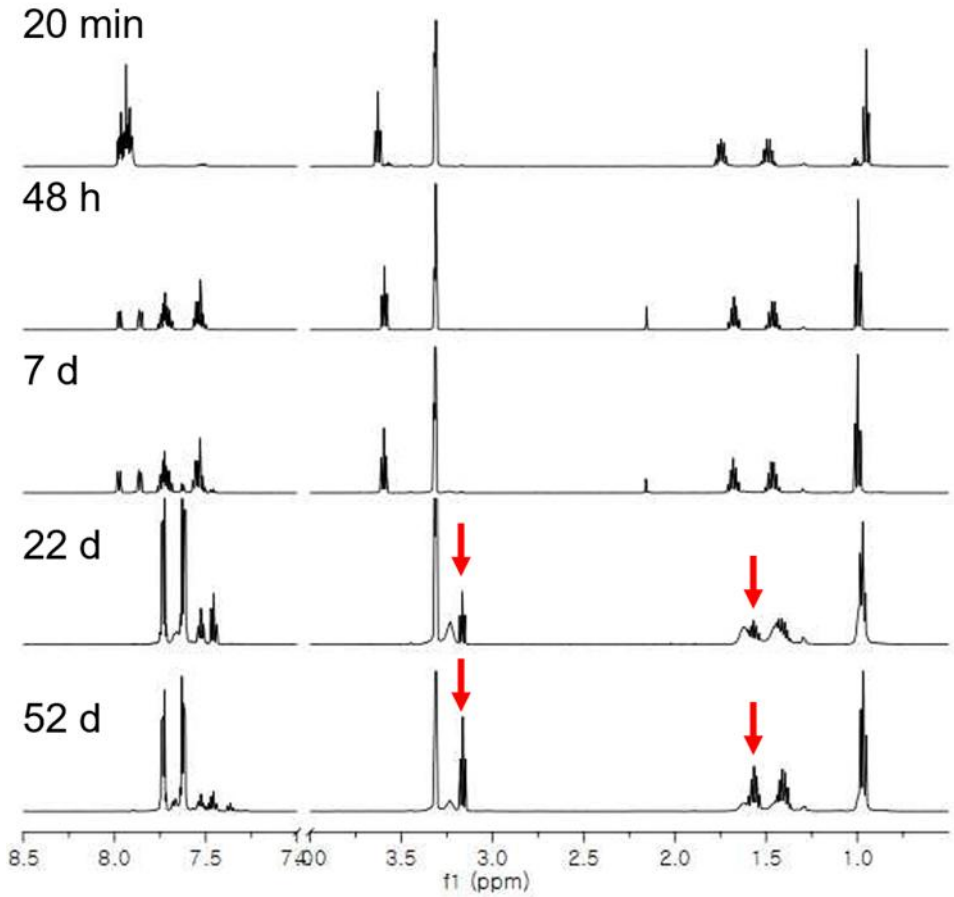

Figure 25. 3ab was incubated in CD_3OD (5 mg/ml, 37 °C) and ^1H-NMR spectra were recorded on Varian NMR System 500 MHz. **3ab** seems to be decomposed to the corresponding guanidine-amic acid within 48 h. The resulting guanidine-amic acid was stable in CD_3OD for several days. Further incubation induced release of butylguanidine (red arrow).

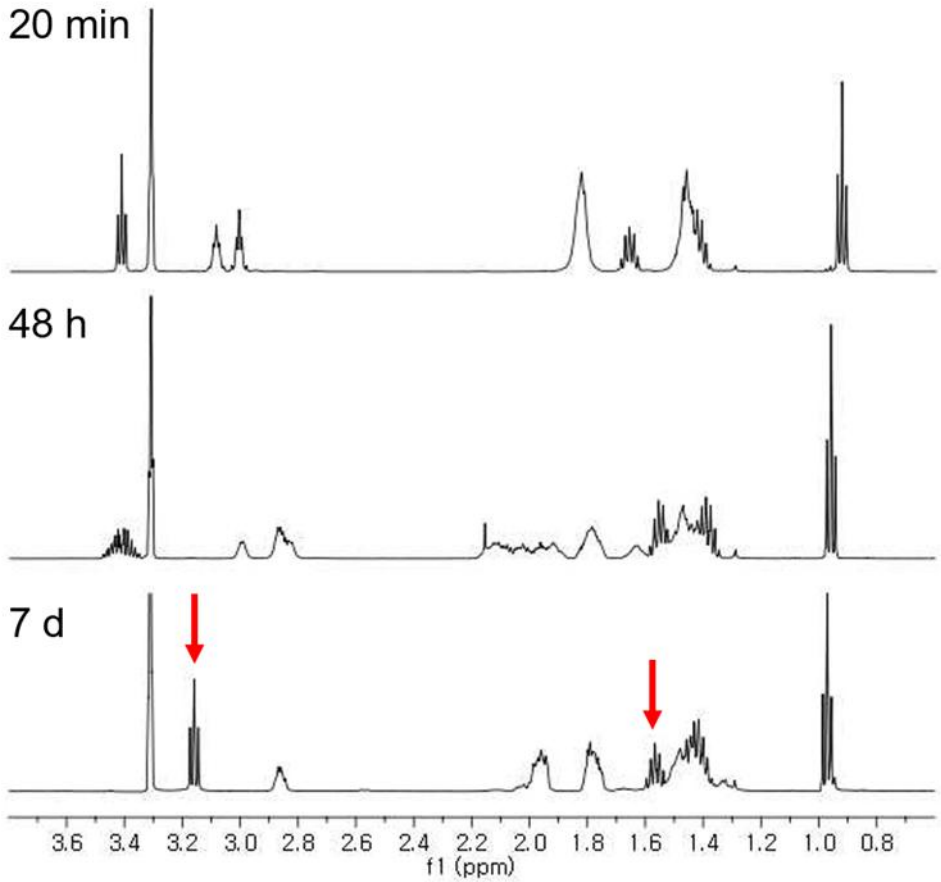

Figure 26. **3ac** was incubated in CD_3OD (5 mg/ml, 37 °C) and ^1H-NMR spectra were recorded on Varian NMR System 500 MHz. Similar to **3ab**, **3ac** seems to be decomposed to yield corresponding guanidine-amic acid within 48 h. After incubation for 7 days, **3ac** completely degraded into butylguanidine (red arrow).

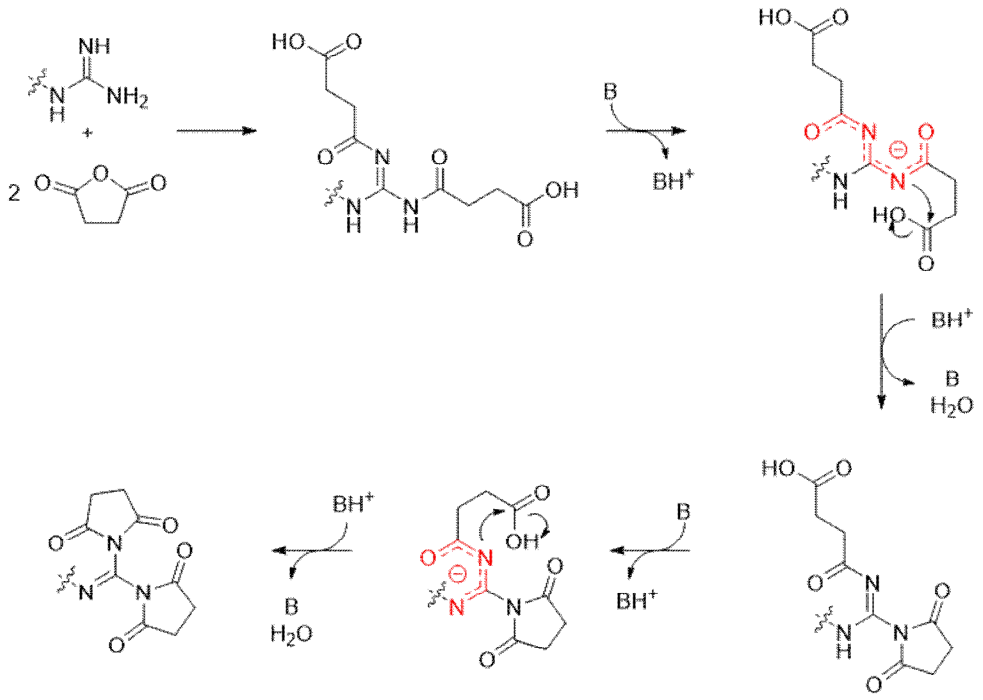

Figure 27. Proposed mechanism for GCDI formations.

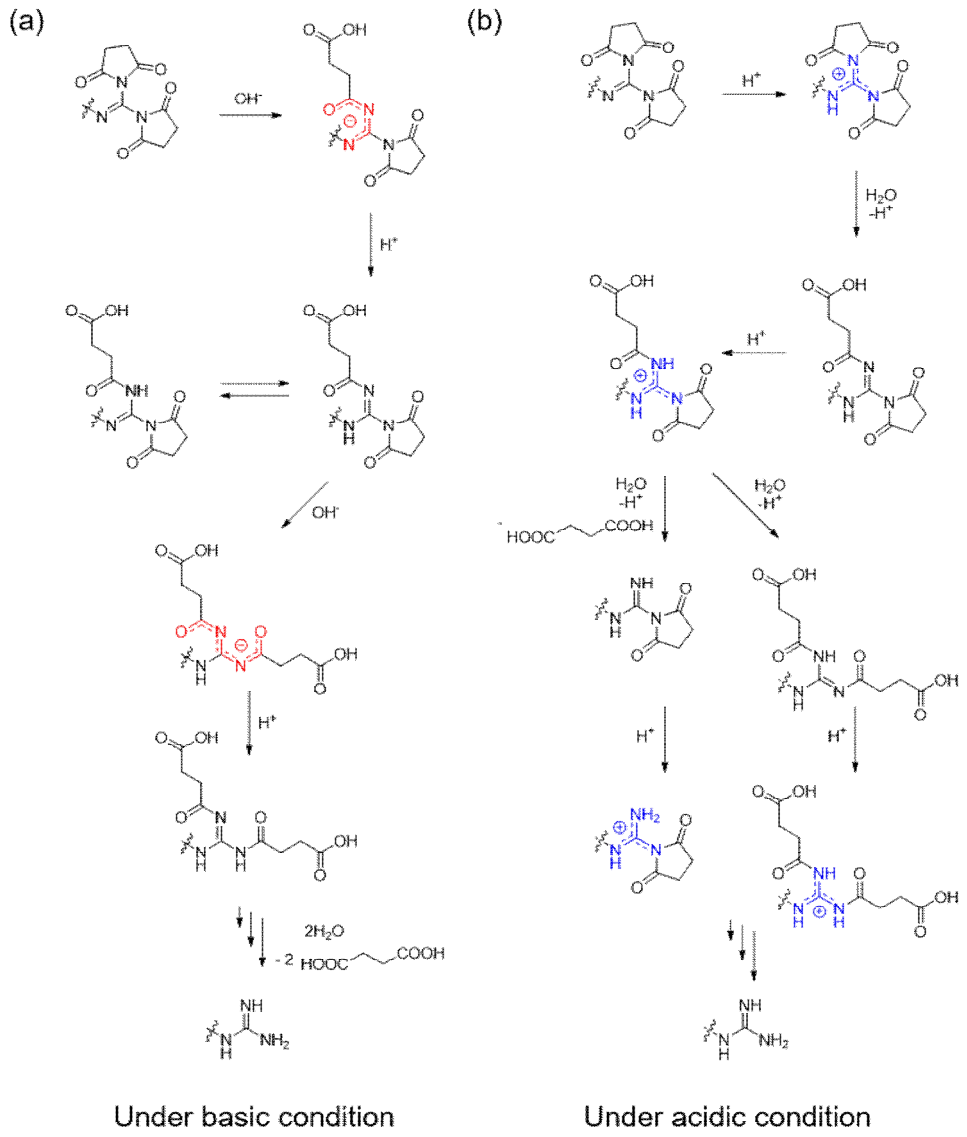

Figure 28. Proposed mechanisms for GCDI degradations under (a) basic and (b) acidic conditions. Resonance-stabilized intermediates were indicated in red and blue, respectively.

Tables

Table 1. Optimization Studies[a]

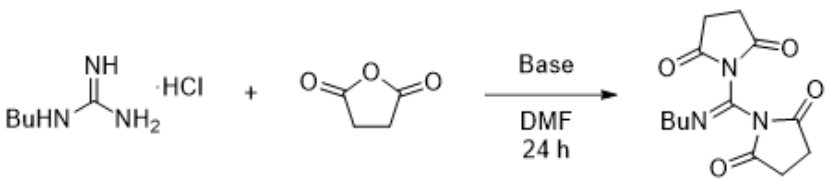

1a **2a** **3aa**

Entry	Base	equiv. of base	equiv. of anhydride	Temperature	Yield[b]
1	TEA	1.0	2.0	RT	10%
2	DIPEA	1.0	2.0	RT	11%
3	Pyridine	1.0	2.0	RT	-
4	K_2CO_3	1.0	2.0	RT	15% (15%)[c]
5	K_2CO_3	1.0	2.0	30 °C	16%
6	K_2CO_3	1.0	2.0	40 °C	15%
7	K_2CO_3	1.0	2.0	70 °C	Trace
8	K_2CO_3	2.0	2.0	30 °C	Trace
9	K_2CO_3	3.0	2.0	30 °C	Trace
10	K_2CO_3	1.0	4.0	30 °C	51%
11	K_2CO_3	1.0	6.0	30 °C	75%
12	K_2CO_3	1.0	8.0	30 °C	85%
13	TEA	15.0	5.0	RT	37%
14	-	-	6.0	RT	-

a) All the reactions were performed on 100 mg scale of butylguanidine hydrochloride (**1a**). b) Isolated yields. c) The yield was calculated by ^{1}H-NMR.

Table 2. Crystal Structure and Structure Refinement for compound **3aa**

Empirical formula	C_{13} H_{17} N_3 O_4
Formula weight	279.29
Temperature	173(2) K
Wavelength	0.71073 Å
Crystal system	Monoclinic
Space group	$P2_1/n$
Unit cell dimensions	a = 9.69440(10) Å
	α = 90°.
	b = 8.73060(10) Å
	β = 94.1674(8)°.
	c = 16.4787(2) Å
	γ = 90°.
Volume	1391.04(3) $Å^3$
Z	4
Density (calculated)	1.334 Mg/m^3
Absorption coefficient	0.100 mm^{-1}
F(000)	592
Crystal size	0.309 x 0.215 x 0.140 mm^3
Theta range for data collection	2.365 to 28.297°.
Index ranges	-12<=h<=11, -10<=k<=11,
	-21<=l<=21
Reflections collected	13751
Independent reflections	3451 [R(int) = 0.1023]
Completeness to theta = 25.242°	100.0 %
Absorption correction	Semi-empirical from
equivalents	

Max. and min. transmission	0.7457 and 0.7011
Refinement method	Full-matrix least-squares on F^2
Data / restraints / parameters	3451 / 0 / 181
Goodness-of-fit on F^2	1.034
Final R indices [I>2sigma(I)]	R1 = 0.0525, wR2 = 0.1386
R indices (all data)	R1 = 0.0650, wR2 = 0.1472
Extinction coefficient	n/a
Largest diff. peak and hole	0.240 and -0.362 e.$Å^{-3}$

Table 3. The optimized atomic coordinates of **3aa** in gas phase at uB3LYP with the 6-31G(d,p) basis set.

Atom	X	Y	Z
C	4.741723	-0.01996	-0.04429
H	4.620233	0.770139	-0.79821
H	4.983087	0.493056	0.896801
C	3.420776	-0.77897	0.116532
H	3.525681	-1.56648	0.872454
H	3.161016	-1.28552	-0.82155
C	2.265745	0.14095	0.520557
H	2.477311	0.621402	1.482939
H	2.150316	0.951668	-0.21478
C	5.903188	-0.93427	-0.44405
H	5.69824	-1.43679	-1.396
H	6.836382	-0.37279	-0.55566
H	6.068317	-1.71204	0.309921
C	-0.06939	-0.21148	0.310397
N	1.051541	-0.63855	0.685364
C	-0.17797	2.24981	0.620111
C	-1.48719	2.827376	-1.34961
C	-0.90457	3.404739	-0.05362
H	-1.01298	3.226056	-2.25158
H	-2.56436	2.973254	-1.45665
H	-0.20708	4.232644	-0.20144
H	-1.67726	3.74592	0.641022
C	-2.47443	-0.64898	0.765238
C	-2.60546	-2.92952	-0.06985
C	-3.44863	-1.78922	0.512852
H	-2.95215	-3.28466	-1.04273
H	-2.54112	-3.79927	0.59072
H	-4.21119	-1.42317	-0.18057
H	-3.95321	-2.03695	1.45004
N	-1.20293	-1.06609	0.346383

N	−0.37723	1.097628	−0.17539
C	−1.20184	−2.36031	−0.23983
C	−1.2106	1.332841	−1.28637
O	−0.25857	−2.88406	−0.77196
O	−2.73091	0.442895	1.228253
O	−1.61175	0.475121	−2.03989
O	0.450089	2.272862	1.65013

요약(국문초록)

구아니딘의 친핵성 반응을 통해 얻어질 수 있는 다양한 분자 구조 중 이미드 형태의 구조는 현재까지 거의 보고된 바가 없다. 이는 대부분의 반응 조건에서 구아니딘이 아민에 비해 강한 염기로 작용하는 반면 약한 친핵체로 작용하며 또한 이미드 형성은 보통 탈수를 촉진하기 위해 고온의 무수 조건에서 진행되기 때문으로 생각된다.

본 연구에서는 상온의 반응 조건에서 독특한 구아니딘 고리형 다이이미드 (GCDI) 구조가 손쉽게 얻어지는 것을 처음으로 보고한다. 구아니딘과 고리형 카복실산 무수물의 반응으로부터 예상치 못하게 GCDI 구조가 주요 생성물로서 높은 수득률로 얻어졌다. NMR 분석과 단결정 X-선 회절 분석을 통해 해당 반응의 생성물이 구아니딘의 두 질소 원자에 석신이미드 고리가 형성된 GCDI 구조를 가지는 것을 확인했다. 흥미롭게도, 두 석신이미드 고리는 거의 직각에 가까운 이면각을 가졌으며 이를 통해 비편재화된 π-오비탈 구조가 붕괴하였을 것이라 예상했다. GCDI 구조의 중심에 있는 구아니딘의 C-N 결합 길이 변화 역시 이를 뒷받침한다. 또한, 두 석신이미드 고리는 상온에서 자유롭게 회전할 수 있는 것으로 보인다.

GCDI는 일반적인 아민 기반의 이미드와 구조적 특징뿐만 아니라 분해 특성에서도 상당한 차이를 보이는 것으로 나타났다. GCDI 구조는 비양성자성 용매에서는 최소 수 주 이상 안정했지만, 물이나 메탄올 등의 양성자성 용매 하에서는 상응하는 아마이드로 빠르게 분해되었으며 최종적으로는 처음의 구아니딘을 방출했다. 또한, GCDI의 분해는 산성과 염기성 조건 둘 다에서 촉진되는 것을 확인했다. 구아니딘 기반의 이미드가 일반적인 아민 기반의 이미드보다 훨씬 손쉽게 형성, 분해되는 것이 구아니딘 구조의 전하 비편재화에 따른 안정화에 기인한다고 추정된다.

주요어: 구아니딘 고리형 다이이미드 (GCDI), 고우시 구조, 가용매 분해,

전하-비편재화 된 중간체

학 번: 2016-29102